

Unbounded-Time Analysis of Guarded LTI Systems with Inputs by Abstract Acceleration

Dario Cattaruzza Alessandro Abate Peter Schrammel Daniel Kroening

Abstract—Reachability analysis of continuous and discrete time systems is a hard problem that has seen much progress in the last decades. In many cases the problem has been reduced to bisimulations with a number of limitations in the nature of the dynamics, soundness, or time horizon. In this article we focus on sound safety verification of Unbounded-Time Linear Time-Invariant (LTI) systems with inputs using reachability analysis. We achieve this by using Abstract Acceleration, which over-approximates the reach tube of a system over unbounded time by using abstraction. The technique is applied to a number of models and the results show good performance when compared to state-of-the-art tools.

I. INTRODUCTION

Linear loops are an ubiquitous programming pattern. Linear loops iterate over continuous variables, which are updated with a linear transformation. Linear loops may be guarded, i.e., terminate if a given linear condition holds. Inputs from the environment can be modelled by means of non-deterministic choices within the loop. These features make linear loops expressive enough to capture the dynamics of many hybrid dynamical models. The usage of such models in safety-critical embedded systems makes linear loops a fundamental target for formal methods.

Many high-level requirements for embedded control systems can be modelled as safety properties, i.e. deciding reachability of certain *bad states*, in which the system exhibits unsafe behaviour. Bad states may, in linear loops, be encompassed by guard assertions.

Reachability in linear programs, however, is a formidable challenge for automatic analysers: the problem is undecidable despite the restriction to linear transformations (i.e., linear dynamics) and linear guards.

The goal of this article is to push the frontiers of unbounded-time reachability analysis: we aim at devising a method that is able to reason soundly about unbounded trajectories. We present a new approach for performing *abstract acceleration*. Abstract acceleration [26], [27], [34] approximates the effect of an arbitrary number of loop iterations (up to infinity) with a single, non-iterative transfer function that is applied to the entry state of the loop (i.e., to the set of initial conditions of the linear dynamics). This article extends the work in [34] to systems with non-deterministic inputs elaborating the details omitted in [39].

The key contributions of this article are:

- 1) We present a new technique to include inputs (non-determinism) in the abstract acceleration of general linear loops.
- 2) We introduce the use of support functions in complex spaces, in order to increase the precision of previous abstract acceleration methods.

II. PRELIMINARIES

A. Linear Loops with Inputs

Simple linear loops are programs expressed in the form:

$$\text{while}(\mathbf{G}\mathbf{x} \leq \mathbf{h}) \quad \mathbf{x} := \mathbf{A}\mathbf{x} + \mathbf{B}\mathbf{u},$$

where $\mathbf{x} \in \mathbb{R}^p$ is a valuation on the state variables, $\psi := \mathbf{G}\mathbf{x} \leq \mathbf{h}$ is a linear constraint on the states (with $\mathbf{G} \in \mathbb{R}^{r \times p}$ and $\mathbf{h} \in \mathbb{R}^r$), $\mathbf{u} \in \mathbb{R}^q$ is a non-deterministic input, and $\mathbf{A} \in \mathbb{R}^{p \times p}$ and $\mathbf{B} \in \mathbb{R}^{p \times q}$ are linear transformations characterising the dynamics of the system. In particular, the special instance where $\psi = \top$ (i.e., “while true”) represents a time-unbounded loop with no guards, for which the discovery of a suitable invariant (when existing) is paramount. As evident at a semantical level, this syntax can be interpreted as the dynamics of a discrete-time LTI model with inputs, under the presence of a guard set which, for ease of notation, we denote as $G = \{\mathbf{x} \mid \mathbf{G}\mathbf{x} \leq \mathbf{h}\}$. In the remaining of this work we will also use the notation $\mathbf{M}_{i,*}$ to represent the rows of a matrix and $\mathbf{M}_{*,j}$ its columns.

B. Model Semantics

The traces of the model starting from an initial set $X_0 \subseteq \mathbb{R}^p$, with inputs restricted to $U \subseteq \mathbb{R}^q$, are sequences $\mathbf{x}_0 \xrightarrow{u_0} \mathbf{x}_1 \xrightarrow{u_1} \mathbf{x}_2 \xrightarrow{u_2} \dots$, where $\mathbf{x}_0 \in X_0$ and $\forall k \geq 0, \mathbf{x}_{k+1} = \tau(\mathbf{x}_k, \mathbf{u}_k)$, where

$$\tau(\mathbf{x}_k, \mathbf{u}_k) = \{\mathbf{A}\mathbf{x}_k + \mathbf{B}\mathbf{u}_k \mid \mathbf{G}\mathbf{x}_k \leq \mathbf{h} \wedge \mathbf{u}_k \in U\} \quad (1)$$

We extend the notation above to convex sets of states and inputs (X and U), and denote the set of states reached from X by τ in one step:

$$\tau(X, U) = \{\tau(\mathbf{x}, \mathbf{u}) \mid \mathbf{x} \in X, \mathbf{u} \in U\} \quad (2)$$

We furthermore denote the set of states reached from X_0 via τ in n steps (*n-reach set*), for $n \geq 0$:

$$\begin{aligned} \tau^0(X_0, U) &= X_0 \\ \tau^n(X_0, U) &= \tau(\tau^{n-1}(X_0, U) \cap G, U) \end{aligned} \quad (3)$$

Since the transformations \mathbf{A} and \mathbf{B} are linear, and vector sums preserve convexity, the sets $X_n = \tau^n(X_0, U)$ are also convex.

We define the *n-reach tube*

$$\hat{X}_n = \hat{\tau}^n(X_0, U) = \bigcup_{k \in [0, n]} \tau^k(X_0, U) \quad (4)$$

as the union of the reachable sets over n iterations. Moreover, $\hat{X} = \bigcup_{n \geq 0} \tau^n(X_0, U)$ extends the previous notion over an unbounded time horizon.

C. Support Functions

1) *Support Function Definition*: A support function is a convex function on \mathbb{R}^p which describes the distance of a supporting hyperplane for a given geometrical set in \mathbb{R}^p .

Support functions may be used to describe a set by defining the distance of its convex hull with respect to the origin, given a number of directions. More specifically, the distance from the origin to the hyperplane that is orthogonal to the given direction and that touches its convex hull at its farthest. Finitely sampled support functions are template polyhedra in which the directions are not fixed, which helps avoiding wrapping effects [25]. The larger the number of directions provided, the more precisely represented the set will be.

In more detail, given a direction $\mathbf{v} \in \mathbb{R}^p$, the support function of a non-empty set $X \subseteq \mathbb{R}^p$ in the direction of \mathbf{v} is defined as

$$\rho_X : \mathbb{R}^p \rightarrow \mathbb{R}, \quad \rho_X(\mathbf{v}) = \sup\{\mathbf{x} \cdot \mathbf{v} : \mathbf{x} \in X\}.$$

where $\mathbf{x} \cdot \mathbf{v} = \sum_{i=0}^p x_i v_i$ is the dot product of the two vectors.

Support functions do not exclusively apply to convex polyhedra, but in fact to any set $X \subseteq \mathbb{R}^p$ represented by a general assertion $\theta(X)$. We will restrict ourselves to the use of convex polyhedra, in which case the support function definition translates to solving the linear program

$$\rho_X(\mathbf{v}) = \max\{\mathbf{x} \cdot \mathbf{v} \mid \mathbf{C}\mathbf{x} \leq \mathbf{d}\}. \quad (5)$$

2) *Support Functions Properties:* Several properties of support functions allow us to reduce operational complexity. The most significant are [23]:

$$\begin{aligned}\rho_{kX}(\mathbf{v}) &= \rho_X(k\mathbf{v}) = k\rho_X(\mathbf{v}) : k \geq 0 \\ \rho_{AX}(\mathbf{v}) &= \rho_X(A^T\mathbf{v}) : A \in \mathbb{R}^{p \times p} \\ \rho_{X_1 \oplus X_2}(\mathbf{v}) &= \rho_{X_1}(\mathbf{v}) + \rho_{X_2}(\mathbf{v}) \\ \rho_X(\mathbf{v}_1 + \mathbf{v}_2) &\leq \rho_X(\mathbf{v}_1) + \rho_X(\mathbf{v}_2) \\ \rho_{\text{conv}(X_1 \cup X_2)}(\mathbf{v}) &= \max\{\rho_{X_1}(\mathbf{v}), \rho_{X_2}(\mathbf{v})\} \\ \rho_{X_1 \cap X_2}(\mathbf{v}) &\leq \min\{\rho_{X_1}(\mathbf{v}), \rho_{X_2}(\mathbf{v})\}\end{aligned}$$

As can be seen by their structure, some of these properties reduce complexity to lower-order polynomial or even to constant time, by turning matrix-matrix multiplications ($O(p^3)$) into matrix-vector ($O(p^2)$), or into scalar multiplications.

3) *Support Functions in Complex Spaces:*

The literature does not state, as far as we found any description of the use of support functions in complex spaces. Since this is relevant to using our technique, we extend the definition of support functions to encompass their operation on complex spaces.

A support function in a complex vector field is a transformation:

$$\rho_X(\mathbf{v}) : \mathbb{C}^p \rightarrow \mathbb{R} = \sup\{|\mathbf{x} \cdot \mathbf{v}| \mid \mathbf{x} \in X \subseteq \mathbb{C}^p, \mathbf{v} \in \mathbb{C}^p\}.$$

The dot product used here is the Euclidean Internal Product of the vectors, which is commonly defined in the complex space as:

$$\mathbf{a} \cdot \mathbf{b} = \sum_{i=0}^p a_i \bar{b}_i, \quad \mathbf{a}, \mathbf{b} \in \mathbb{C}^p$$

We are interested in the norm of the complex value, which is a 1-norm given our definition of dot product:

$$|\mathbf{a} \cdot \mathbf{b}| = |\text{re}(\mathbf{a} \cdot \mathbf{b})| + |\text{im}(\mathbf{a} \cdot \mathbf{b})|$$

Returning to our support function properties, we now have:

$$\rho_X(re^{i\theta}\mathbf{v}) = r\rho_X(e^{i\theta}\mathbf{v}),$$

which is consistent with the real case when $\theta = 0$. The reason why $e^{i\theta}$ cannot be extracted out is because it is a rotation, and therefore follows the same rules as a matrix multiplication,

$$\rho_X(e^{i\theta}\mathbf{v}) \triangleq \rho_X \left(\begin{bmatrix} \cos \theta & \sin \theta \\ -\sin \theta & \cos \theta \end{bmatrix} \mathbf{v} \right).$$

Since matrices using pseudo-eigenvalues are real, all other properties remain the same. An important note is that when using pseudo-eigenvalues, conjugate eigenvector pairs must be also converted into two separate real eigenvectors, corresponding to the real and the imaginary parts of the pair.

III. THE POLYHEDRAL ABSTRACT DOMAIN

A. Convex Polyhedra

A polyhedron is a topological element in \mathbb{R}^p with flat polygonal (2-dimensional) faces. Each face corresponds to a hyperplane that creates a halfspace, and the intersections of these hyperplanes are the edges of the polyhedron. A polyhedron is said to be convex if its surface does not intersect itself and a line segment joining any two points of its surface is contained in the interior of the polyhedron. Convex polyhedra are better suited than general polyhedra as an abstract domain, mainly because they have a simpler representation and operations over convex polyhedra are in general easier than for general polyhedra. There are a number of properties of convex polyhedra that make them ideal for abstract interpretation of continuous spaces, including their ability to reduce an uncountable set of real points into a countable set of faces, edges and vertices. Convex polyhedra retain their convexity across linear transformations, and are functional across a number of operations because they have a dual representation [21]. The mechanism to switch between these two representations is given in section III-B5

1) *Vertex Representation:* Since every edge in the polyhedron corresponds to a line between two vertices and every face corresponds to the area enclosed

by a set of co-planar edges, a full description of the polyhedron is obtain by simply listing its vertices. Since linear operations retain the topological properties of the polyhedron, performing these operations on the vertices is sufficient to obtain a complete description of the transformed polyhedron (defined by the transformed vertices). Formally, a polyhedron is a set $V \in \mathbb{R}^p$ such that $\mathbf{v} \in V$ is a vertex of the polyhedron.

2) *Inequality Representation:* The dual of the Vertex representation is the face representation. Each face corresponds to a bounding hyperplane of the polyhedron (with the edges being the intersection of two hyperplanes and the vertices the intersection of 3 or more), and described mathematically as a function of the vector normal to the hyperplane. If we examine this description closely, we can see that it corresponds to the support function of the vector normal to the hyperplane. Given this description we formalise the following: A convex polyhedron is a topological region in \mathbb{R}^p described by the set

$$X = \{\mathbf{x} \in \mathbb{R}^p \mid \mathbf{C}\mathbf{x} \leq \mathbf{d}, \mathbf{C} \in \mathbb{R}^{m \times p}, \mathbf{d} \in \mathbb{R}^m\}$$

where the rows $\mathbf{C}_{i,*}$ for $i \in [1, m]$ correspond to the transposed vectors normal to the faces of the polyhedron and \mathbf{d}_i for $i \in [1, m]$ their support functions. For simplicity of expression, we will extend the use of the support function operator as follows:

$$\rho'_X : \mathbb{R}^{m \times p} \rightarrow \mathbb{R}^m$$

$$\rho'_X(\mathbf{M}^T) = \begin{bmatrix} \rho_X(\mathbf{M}_{1,*}^T) \\ \rho_X(\mathbf{M}_{2,*}^T) \\ \vdots \\ \rho_X(\mathbf{M}_{m,*}^T) \end{bmatrix}$$

B. Operations on Convex Polyhedra

Several operations of interest can be performed on convex polyhedra

1) *Translation:* Given a vertex representation V and a translation vector \mathbf{t} , the transformed polyhe-

dron is

$$V' = \{\mathbf{v}' = \mathbf{v} + \mathbf{t} \mid \mathbf{v} \in V\}$$

Given an inequality representation X and a translation vector \mathbf{t} , the transformed polyhedron corresponds to

$$X' = \{\mathbf{x} \mid \mathbf{C}\mathbf{x} \leq \mathbf{d} + \mathbf{C}\mathbf{t}\}$$

2) *Linear Transformation:* Given a vertex representation V and a linear transformation \mathbf{L} , the transformed polyhedron is

$$V' = \mathbf{L}V$$

Given an inequality representation X and a linear transformation \mathbf{L} , the transformed polyhedron corresponds to

$$X' = \{\mathbf{x} \mid \mathbf{C}(\mathbf{L}^+)^T \mathbf{x} \leq \rho'_X(\mathbf{L}^+ \mathbf{C}^T)\}$$

where \mathbf{L}^+ represents the pseudo-inverse of \mathbf{L} . In the case when the inverse \mathbf{L}^{-1} exists, then

$$X' = \{\mathbf{x} \mid \mathbf{C}(\mathbf{L}^{-1})^T \mathbf{x} \leq \mathbf{d}\}$$

From this we can conclude that linear transformations are better handled by a vertex representation, except when the inverse of the transformation exists and is know a-priori. This works makes use of this last case to avoid continuous swapping in representations.

3) *Set Sums:* The addition of two polyhedra is a slightly more complex matter. The resulting set is one such that for all possible combinations of points inside both original polyhedra, the sum is contained in the result. This operation is commonly known as the Minkowski sum, namely

$$A \oplus B = \{a + b \mid a \in A, b \in B\}$$

Given two vertex representations V_1 and V_2 the resulting polyhedron

$$V = \text{conv}(V_1 \oplus V_2)$$

where $\text{conv}(\cdot)$ is the convex hull of the set of vertices contained in the Minkowski sum.

Let

$$\begin{aligned} X_1 &= \{\mathbf{x} \mid \mathbf{C}_1 \mathbf{x} \leq \mathbf{d}_1\} \\ X_2 &= \{\mathbf{x} \mid \mathbf{C}_2 \mathbf{x} \leq \mathbf{d}_2\} \end{aligned}$$

be two sets, then

$$X = X_1 \oplus X_2 = \{\mathbf{x} \mid \mathbf{C} \mathbf{x} \leq \mathbf{d}\},$$

where

$$\mathbf{C} = \begin{bmatrix} \mathbf{C}_1 \\ \mathbf{C}_2 \end{bmatrix}, \quad \mathbf{d} = \begin{bmatrix} \mathbf{d}_1 + \rho'_{X_2}(\mathbf{C}_1^T) \\ \mathbf{d}_2 + \rho'_{X_1}(\mathbf{C}_2^T) \end{bmatrix}.$$

Because these sets correspond to systems of inequalities, they may be reduced removing redundant constraints. Note that if $\mathbf{C}_1 = \mathbf{C}_2$ then

$$X = X_1 \oplus X_2 = \{\mathbf{x} \mid \mathbf{C}_1 \mathbf{x} \leq \mathbf{d}_1 + \mathbf{d}_2\},$$

4) Set Hadamard Product:

Lemma 1. *Given two vertex representations V_1 and V_2 the resulting polyhedron*

$$V = V_1 \circ V_2 = \text{conv}(\{\mathbf{v} = \mathbf{v}_1 \circ \mathbf{v}_2 \mid \mathbf{v}_1 \in V_1, \mathbf{v}_2 \in V_2\})$$

where \circ represents the Hadamard (coefficient-wise) product of the vectors, contains all possible combinations of products between elements of each set.

Proof: Given a convex set X , we have:

$$X' = \{\mathbf{x}_{ij} \mid \mathbf{x}_i, \mathbf{x}_j \in X, \mathbf{x}_{ij} = t\mathbf{x}_i + (1-t)\mathbf{x}_j, t \in [0, 1]\} \subseteq X$$

Given $\mathbf{x}_i \in X$, $\mathbf{y}_j \in Y$, $\mathbf{z}_{i,j} = \mathbf{x}_i \circ \mathbf{y}_j \in Z$

$$\mathbf{x}_{ij} \in X', \mathbf{y}_k \in Y, \mathbf{z}_{i,k}, \mathbf{z}_{j,k} \in Z \Rightarrow \mathbf{z}_{i,j,k} \in Z$$

$$\mathbf{x}_{ij} \in X, \mathbf{y}_m, \mathbf{y}_n \in Y, \mathbf{z}_{ij,m}, \mathbf{z}_{ij,n} \in Z \Rightarrow \mathbf{z}_{ij,mn} \in Z$$

This equation proves that given $\mathbf{v}_{11}, \mathbf{v}_{12} \in V_1$, $\mathbf{v}_{21}, \mathbf{v}_{22} \in V_2$ and $u, t \in [0, 1]$,

$$(t\mathbf{v}_{11} + (1-t)\mathbf{v}_{12})(u\mathbf{v}_{21} + (1-u)\mathbf{v}_{22}) \in V$$

5) *Vertex Enumeration:* The vertex enumeration problem corresponds to the algorithm required to obtain a list of all vertices of a polyhedron given an inequality description of its bounding hyperplanes. Given the duality of the problem, it is also possible to find the bounding hyperplanes given a vertex description if the chosen algorithm exploits this duality. In this case the description of V is given in the forms of a matrix inequality $\mathbf{V} \mathbf{x} \leq [1 \ 1 \ \dots \ 1]^T$ with $\mathbf{V} = [\mathbf{v}_1 \ \dots \ \mathbf{v}_m]^T, \mathbf{v}_i \in V$. Similarly, A can be described as a set containing each of its rows. At the time of writing, there are two algorithms that efficiently solve the vertex enumeration problem. Irs is a reverse search algorithm, while cdd follows the double description method. In this work we use the cdd algorithm for convenience in implementation (the original cdd was developed for floats, whereas Irs uses rationals). The techniques presented here can be applied to either.

Let

$$C = \{\mathbf{x} \mid \mathbf{A} \mathbf{x} \geq 0, \mathbf{A} \in \mathbb{R}^{n \times p}, \mathbf{x} \in \mathbb{R}^p\}$$

be the polyhedral cone represented by A . The pair (A, V) is said to be a double description pair if

$$C = \{\lambda^T V \mid V \in \mathbb{R}^p, \lambda \in \mathbb{R}_{\geq 0}^{|V|}\}$$

V is called the generator of X . Each element in V lies in the cone of X , and its minimal form (smallest m) has a one-to-one correspondence with the extreme rays of X if the cone is pointed (i.e., it has a vertex at the origin). This last can be ensured by translating a polyhedral description so that it includes the origin, and then translating the vertices back once they have been discovered (see section III-B).

We will also point out that

$$\{\mathbf{x} \mid \mathbf{A} \mathbf{x} \leq \mathbf{b}\} = \{\mathbf{x}' \mid [-\mathbf{A} \ \mathbf{b}] \mathbf{x}' \geq 0\}$$

$$\text{where } \mathbf{x} \in \mathbb{R}^p \text{ and } \mathbf{x}' = \begin{bmatrix} \mathbf{x} \\ 1 \end{bmatrix} \in \mathbb{R}^{p+1}.$$

The vertex enumeration algorithm starts by finding

■ a base C_K which contains a number of vertices of

the polyhedron. This can be done by pivoting over a number of different rows in \mathbf{A} and selecting the feasible visited points, which are known to be vertices of the polyhedron (pivoting p times will ensure at least one vertex is visited if the polyhedron is non-empty). C_K is represented by \mathbf{A}_K which contains the rows used for the pivots. The base C_K is then iteratively expanded to C_{K+i} by exploring the i^{th} row of \mathbf{A} until $C_K = C$. The corresponding pairs $(\mathbf{A}_{K+i}, V_{K+i})$ are constructed using the information from (\mathbf{A}_K, V_K) as follows:

Let $\mathbf{A}_K \in \mathbb{R}^{n_K \times p}$, $\mathbf{A}_{i,*} \in \mathbb{R}^{1 \times p}$, $V_K \in \mathbb{R}^p$,

$$H_i^+ = \{\mathbf{x} \mid \mathbf{A}_{i,*}\mathbf{x} > 0\}, \quad (6)$$

$$H_i^- = \{\mathbf{x} \mid \mathbf{A}_{i,*}\mathbf{x} < 0\}, \quad (7)$$

$$H_i^0 = \{\mathbf{x} \mid \mathbf{A}_{i,*}\mathbf{x} = 0\} \quad (8)$$

be the spaces outside inside and on the i^{th} hyperplane and

$$V_K^+ = \{\mathbf{v}_j \in H_i^+\}, \quad (9)$$

$$V_K^- = \{\mathbf{v}_j \in H_i^-\}, \quad (10)$$

$$V_K^0 = \{\mathbf{v}_j \in H_i^0\} \quad (11)$$

the existing vertices lying on each of these spaces. Then

$$V_{K+i} = V_K^+ \cup V_K^- \cup V_K^0 \cup V_K^i \quad (12)$$

$$V_K^i = \{(\mathbf{A}_{i,*}\mathbf{v}^+)\mathbf{v}^- - (\mathbf{A}_{i,*}\mathbf{v}^-)\mathbf{v}^+ \mid \mathbf{v}^- \in V^-, \mathbf{v}^+ \in V^+\} \quad (13)$$

For the proof see [21].

IV. ABSTRACT MATRICES IN ABSTRACT ACCELERATION

A. Acceleration Techniques

Acceleration of a transition system is a method that seeks to precisely describe the transition relations over a number of steps using a concise description of the overall transition between the first and final step. Namely, it looks for a direct formula to calculate the postimage of a loop from the initial states of the loop. Formally, given the dynamics in equation (1) an acceleration formula aims at

computing the reachset (3) using a function f such that $f(\cdot) = \tau^n(\cdot)$. In the case of systems without inputs, this equation is $\mathbf{x}_n = \mathbf{A}^n \mathbf{x}_0$. We will use this property and others derived from it to calculate our abstract matrices.

B. Overview of the Algorithm

The basic steps required to evaluate a reach tube using abstract acceleration can be seen in figure 1.

- 1) The process starts by doing eigendecomposition of the dynamics (\mathbf{A}) in order to transform the problem into a simpler one.
- 2) A variety of off-the-shelf tools may be used, but since larger problems require numerical algorithms for scalability, a second step involves upper-bounding the error in order to obtain sound results. In such cases, all subsequent steps must be performed using interval arithmetic.
- 3) The inverse of the generalised eigenvectors must be calculated soundly.
- 4) The problem gets transformed into canonical form by multiplying both sides of the equation by \mathbf{S}^{-1} :

$$\mathbf{X}'_k = \mathbb{J}(\mathbf{X}'_{k-1} \cap \mathbf{G}') + \mathbf{U}' \text{ where}$$

$$\mathbf{X}' = \mathbb{S}^{-1}\mathbf{X}, \mathbf{U}' = \mathbb{S}^{-1}\mathbf{B}\mathbf{U} \text{ and } \mathbf{G}' = \{\mathbf{x} \mid \mathbf{G}\mathbb{S}\mathbf{x} \leq \mathbf{h}\}$$

- 5) We calculate the number of iterations as explained in section VI. If there are no guards, we use $n = \infty$. It is worth noting that this number need not be exact: if we overapproximate the number of iterations, the resulting reachtube will overapproximate the desired one.
- 6) we overapproximate the dynamics of the variable inputs (for parametric or no inputs this step will be ignored) using the techniques described in section V-D
- 7) we calculate the abstract dynamics using the techniques described in section V-A

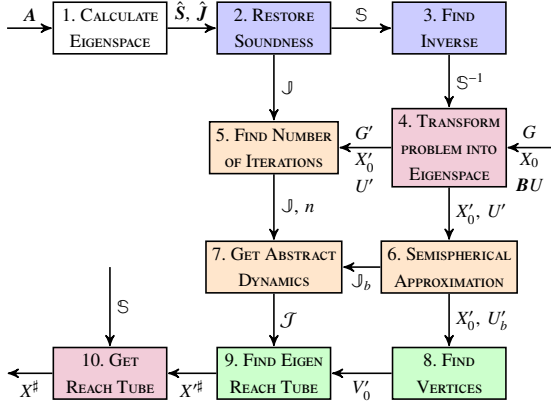


Fig. 1. Block diagram describing the different steps used to calculate the abstract reach tube of a system.

- 8) we evaluate the vertices of the combined input-initial eigenspace to be used as source for the reachtube calculation
- 9) we use a sound simplex algorithm to evaluate the convex set product of the abstract dynamics (used as the tableau) and the initial set (whose vertices are used as the objective functions alongside a set of template directions for the result).
- 10) since we have calculated our result in the eigenspace, we transform the reachtube back into the normal space by multiplying by \mathbb{S} .

C. Computation of Abstract Matrices

We define the abstract matrix \mathcal{A}^n as an over-approximation of the union of the powers of the matrix A^k such that $\mathcal{A}^n \supseteq \bigcup_{k \in [0, n]} A^k$ and its application to the initial set X_0

$$\hat{X}_n^\# = \mathcal{A}^n X_0 \supseteq \hat{X}_n \quad (14)$$

Next we explain how to compute such an abstract matrix. For simplicity, we first describe this computation for matrices A with real eigenvalues, whereas the extension to the complex case will be addressed in Section IV-D. Similar to [34], we first have to compute the Jordan normal form of A . Let $A = \mathbf{S}\mathbf{J}\mathbf{S}^{-1}$ where \mathbf{J} is the normal Jordan form of A , and \mathbf{S} is

made up by the corresponding eigenvectors. We can then easily compute $A^n = \mathbf{S}\mathbf{J}^n\mathbf{S}^{-1}$, where

$$\mathbf{J}^n = \begin{bmatrix} \mathbf{J}_1^n & & \\ & \ddots & \\ & & \mathbf{J}_r^n \end{bmatrix} \quad (15)$$

$$\mathbf{J}_{s \in [1, r]}^n = \begin{bmatrix} \lambda_s^n & \binom{n}{1} \lambda_s^{n-1} & \dots & \binom{n}{p_s-1} \lambda_s^{n-p_s+1} \\ & \lambda_s^n & \binom{n}{1} \lambda_s^{n-1} & \vdots \\ \vdots & & \ddots & \vdots \\ & & & \lambda_s^n \end{bmatrix} \quad (16)$$

The abstract matrix \mathcal{A}^n is computed as an abstraction over a set of vectors $\mathbf{m}^k \in \mathbb{R}^p, k \in [1, n]$ of entries of \mathbf{J}^k .

Let $\mathbf{I}_s = [1 \ 0 \ \dots \ 0] \in \mathbb{R}^{p_s}$. The vector \mathbf{m}^k is obtained by the transformation φ^{-1} :

$$\mathbf{m}^k = [\mathbf{I}_1 \mathbf{J}_1^k \ \dots \ \mathbf{I}_r \mathbf{J}_r^k] \in \mathbb{R}^p \quad (17)$$

such that $\mathbf{J}^k = \varphi(\mathbf{m}^k)$.

If \mathbf{J} is diagonal [34], then \mathbf{m}^k equals the vector of powers of eigenvalues $[\lambda_1^k, \dots, \lambda_r^k]$. An interval abstraction can thus be simply obtained by computing the intervals $[\min\{\lambda_s^0, \lambda_s^n\}, \max\{\lambda_s^0, \lambda_s^n\}]$, $s \in [1, r]$. We observe that the spectrum of the interval matrix $\sigma(\mathcal{A}^n)$ (defined as intuitively) is an over-approximation of $\bigcup_{k \in [0, n]} \sigma(A^k)$.

In the case of the s^{th} Jordan block \mathbf{J}_s with geometric non-trivial multiplicity p_s ($\lambda_i = \lambda_{i-1} = \dots$), observe that the first row of \mathbf{J}_s^n contains all (possibly) distinct entries of \mathbf{J}_s^n . Hence, in general, the vector section \mathbf{m}_s is the concatenation of the (transposed) first row vectors $\left(\lambda_s^n, \binom{n}{1} \lambda_s^{n-1}, \dots, \binom{n}{p_s-1} \lambda_s^{n-p_s+1} \right)^T$ of \mathbf{J}_s^n .

Since the transformation φ transforms the vector \mathbf{m} into the shape of (16) of \mathbf{J}^n , it is called a *matrix shape* [34]. We then define the abstract matrix as

$$\mathcal{A}^n = \{ \mathbf{S} \varphi(\mathbf{m}) \mathbf{S}^{-1} \mid \Phi \mathbf{m} \leq \mathbf{f} \}, \quad (18)$$

where the constraint $\Phi \mathbf{m} \leq \mathbf{f}$ is synthesised from intervals associated to the individual eigenvalues and

to their combinations. More precisely, we compute polyhedral relations: for any pair of eigenvalues (or binomials) within \mathbf{J} , we find an over-approximation of the convex hull containing the points

$$\{\mathbf{m}^k \mid k \in [1, n]\} \subseteq \{\mathbf{m} \mid \Phi \mathbf{m} \leq \mathbf{f}\}$$

D. Abstract Matrices in Complex Spaces

To deal with complex numbers in eigenvalues and eigenvectors, [34] employs the real Jordan form for conjugate eigenvalues $\lambda = re^{i\theta}$ and $\lambda^* = re^{-i\theta}$ ($\theta \in [0, \pi]$), so that

$$\begin{bmatrix} \lambda & 0 \\ 0 & \lambda^* \end{bmatrix} \text{ is replaced by } r \begin{bmatrix} \cos \theta & \sin \theta \\ -\sin \theta & \cos \theta \end{bmatrix}.$$

Although this equivalence will be of use once we evaluate the progression of the system, calculating powers under this notations is often more difficult than handling directly the original matrices with complex values.

In Section IV-C, in the case of real eigenvalues we have abstracted the entries in the power matrix \mathbf{J}_s^n by ranges of eigenvalues $[\min\{\lambda_s^0 \cdots \lambda_s^n\} \quad \max\{\lambda_s^0 \cdots \lambda_s^n\}]$. In the complex case we can do something similar by rewriting eigenvalues into polar form $\lambda_s = r_s e^{i\theta_s}$ and abstracting by $[\min\{r_s^0 \cdots r_s^n\} \quad \max\{r_s^0 \cdots r_s^n\}] e^{i[0, \min(\theta_s, 2\pi)]}$.

V. GENERAL ABSTRACT ACCELERATION WITH INPUTS

A. Using Support Functions on Abstract Acceleration

As an improvement over [34], the rows in Φ and \mathbf{f} (see (18)) are synthesised by discovering support functions in these sets. The freedom of directions provided by these support functions results in an improvement over the logahedral abstractions used in previous works (see Figures 2 - 5). The mechanism by which this works follows the convex properties of the exponential progression. There are four cases to consider ¹:

¹these explain in detail the procedure alluded in [8]

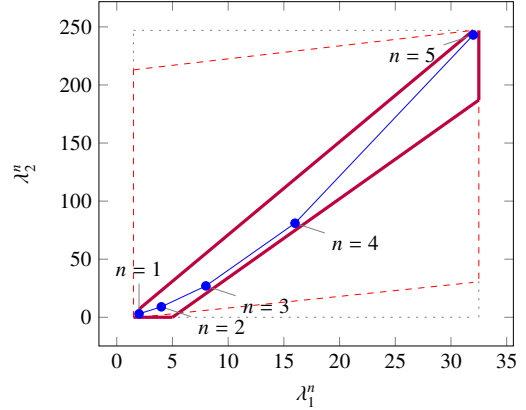


Fig. 2. Polyhedral faces from an \mathbb{R}^2 subspace, where $(\lambda_1^n, \lambda_2^n)$ so that $\lambda_1=2, \lambda_2=3, 1 \leq n \leq 5$. Bold purple lines represent supports found by this article. The dotted grey and dashed red polytopes show logahedral approximations (box and octagon) used in [34]. Note the scales (sloped dashed lines are parallel to the x=y line, and dashed red polytope hides two small faces yielding an octagon).

1) Positive Real Eigenvalues

The exponential curve is cut along the diagonal between the maximum and minimum eigenvalues to create a support function for the corresponding hyperplane. A third point taken from the curve is used to test the direction of the corresponding template vector. An arbitrary number of additional hyperplanes are selected by picking pairs of adjacent points in the curve and creating the corresponding support function as shown in Figure 2.

2) Complex Conjugate Eigenvalue pairs

In the case of complex conjugate pairs, the eigenvalue map corresponds to a logarithmic spiral. In this case, we must first extract the number of iterations required for a full cycle. For convergent eigenvalues, only the first n iterations have an effect on the support functions, while in the divergent case only the last n iterations are considered. Support functions are found for adjacent pairs, checking for the location of the origin point (first point for convergent eigenvalues, last for divergent eigenvalues).

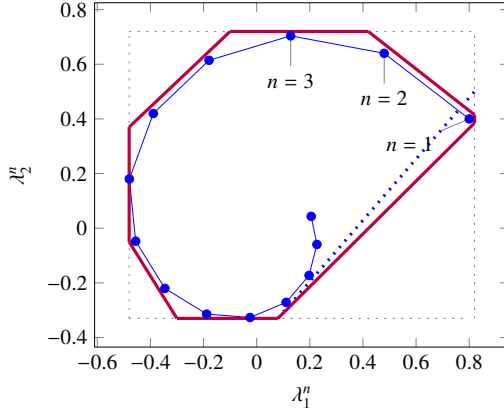


Fig. 3. Polyhedral faces from an \mathbb{R}^2 complex conjugate subspace, where $(\lambda_1^n, \lambda_2^n)$ so that $\lambda_1=0.8+0.4i, \lambda_2=0.8-0.4i, 1 \leq n \leq 14$. Bold purple lines represent supports found by this article. The blue dotted line shows the support function that excludes the origin ($n=1$), which is replaced by the support function projecting from said origin.

If the origin falls outside the support function, we look for an interpolant point that closes the spiral tangent to the origin. This last check is performed as a binary search over the remaining points in the circle (whose supporting planes would exclude the origin) to achieve maximum tightness (see Figure 3).

3) Equal Eigenvalues

When two eigenvalues are the same, the resulting support functions are those orthogonal to the $x = y$ plane, intersecting the square created by the maximum and minimum values.

4) Jordan Blocks of size > 1

In the case of eigenvalues with geometric multiplicities > 1 , the shape of the function is similar to its corresponding unit size block. In the convergent case, since the convexity can be sharp, it is important to find the apex of the upper diagonals in order to minimise the over-approximation. See Figure 4.

5) Negative Eigenvalues and mixed types

When mapping a positive real eigenvalue to a complex conjugate or negative one, we must

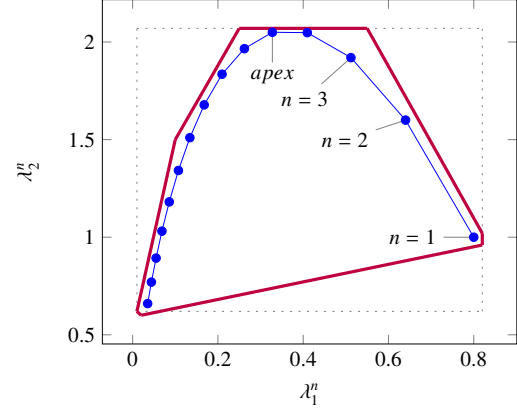


Fig. 4. Polyhedral faces from an \mathbb{R}^2 Jordan block subspace, where $(\lambda_1^n, \lambda_2^n)$ so that $\lambda_1=0.8, \lambda_2=0.8, 1 \leq n \leq 15$. Bold purple lines represent supports found by this article. The blue dotted line shows the support function that excludes the origin ($n=1$), which is replaced by the support function projecting from said origin.

account for both sides of the axis on the latter. These form mirror images that are merged during the abstraction. To make matters simple, we use the magnitude of a complex eigenvalue and evaluate whether the dynamics are concave or convex with respect to the mirroring plane. See Figure 5.

Note that if both eigenvalues are negative and/or conjugate pairs from a different pair, the mirror image would be taken on both axes, resulting in a hyperrectangle. For a tighter bound in the purely convergent case, we find the convex hull of a point cloud for a small time horizon and merge it with the hyperrectangle for the infinite time horizon thereon.

An additional drawback of [34] is that calculating the exact Jordan form of any matrix is computationally expensive and hard to achieve for large-dimensional matrices. We will instead use numerical algorithms in order to get an approximation of the Jordan normal form and account for numerical errors. In particular, if we examine the nature of (14), we find out that the numerical operations are not iterative, therefore the errors do not accumulate with

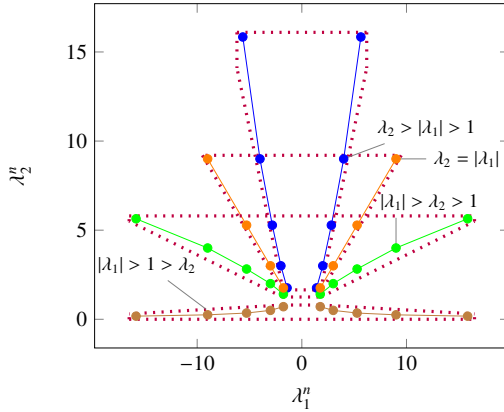


Fig. 5. Polyhedral faces from an \mathbb{R}^2 subspace, with different convexities (note that the blue and orange plots are convex w.r.t. the λ_2^n -axis, whereas the green and brown are concave). Dotted purple lines represent supports for some of these layouts.

time. We use properties of eigenvalues to relax f by finding the maximum error in the calculations that can be determined by computing the norm $\delta_{max} = |\mathbb{A} - \hat{\mathbb{S}}\hat{\mathbb{J}}\mathbb{S}^{-1}|$, where $\hat{\mathbb{J}}$ and $\hat{\mathbb{S}}$ are the numerically calculated eigenvalues and eigenvectors of \mathbb{A} . The notation above is used to represent the matrices as interval matrices and all operations are performed using interval arithmetic with outward rounding in order to ensure soundness. In the following we will presume exact results and use the regular notation to describe the algorithms. The constraints $\Phi\mathbf{m} < f$ are then computed by considering the ranges of eigenvalues $\lambda_s \pm \delta_{max}$ (represented in Fig. 2 as the diameter of the blue dots). The outward relaxation of the support functions (f), which follows a principle similar to that introduced in [22], reduces the tightness of the over-approximation, but ensures the soundness of the abstract matrix \mathcal{A}^n obtained. It is also worth noting that the transformation matrices into and from the eigenspace will also introduce over-approximations due to the intervals. One can still use exact arithmetic with a noticeable improvement over previous work; however, for larger-scale systems the option of using floating-point arithmetic, while taking into account errors and meticulously setting rounding modes, pro-

vides a 100-fold plus improvement, which can make a difference towards rendering verification practically feasible. For a full description on the numerical processes described here see [9]

B. Abstract Matrices in Support Functions

Since we are describing operations using abstract matrices and support functions, we briefly review the nature of these operations and the properties that the support functions retain within this domain. Let $X \in \mathbb{R}^p$ be a space and $\mathcal{A} \in \mathcal{R}^{p \times p}$ an abstract matrix for the same space. From the definition we have

$$\mathcal{A} = \bigcup \mathcal{S}\varphi(\mathbf{m})\mathcal{S}^{-1} : \Phi\mathbf{m} \leq f$$

which leads to

$$\rho_{\mathcal{A}X}(\mathbf{v}) = \rho_{\mathcal{S}\varphi(\mathbf{m})\mathcal{S}^{-1}X}(\mathbf{v}) = \rho_{\varphi(\mathbf{m})\mathcal{S}^{-1}X}(\mathcal{S}^T \mathbf{v}), \quad (19)$$

where

$$\rho_{\varphi X}(\mathbf{v}) = \sup \{ \rho_{\varphi}(\mathbf{x} \circ \mathbf{v}) \mid \mathbf{x} \in X \} \quad (20)$$

and

$$\rho_{\varphi}(\mathbf{v}) = \sup \{ \mathbf{m} \cdot \varphi^{-1}(\mathbf{v}) \mid \Phi\mathbf{m} \leq f \} \quad (21)$$

Here, $\mathbf{x} \circ \mathbf{y}$ is the Hadamard product, where $(\mathbf{x} \circ \mathbf{y})_i = x_i y_i$, and $\varphi^{-1}(\cdot)$ is the reverse operation of $\varphi(\cdot)$ in order to align the elements on \mathbf{v} with the elements in \mathbf{m} . In the case of conjugate pairs this is equivalent to multiplying the vector section by $\begin{bmatrix} 1 & 1 \\ 1 & -1 \end{bmatrix}$, and in the case of a Jordan block by an upper triangular matrix of all ones.

We may also define

$$\begin{aligned} \rho_{\mathcal{A}X}(\mathbf{v}) &= \sup \{ \rho_{aX}(\mathbf{v}), \forall a \in \mathcal{A} \} \\ &= \sup \{ \mathcal{S}\varphi(\mathbf{m})\mathcal{S}^{-1} \mathbf{x} \cdot \mathbf{v}, \forall \mathbf{x} \in X \} \\ &= \sup \{ \varphi(\mathbf{m})\mathcal{S}^{-1} \mathbf{x} \cdot \mathcal{S}^T \mathbf{v}, \forall \mathbf{x} \in X \} \\ &= \sup \{ \rho_{\varphi}(\mathcal{S}^{-1} \mathbf{x} \circ \mathcal{S}^T \mathbf{v}), \forall \mathbf{x} \in X \}. \end{aligned} \quad (22)$$

In order to simplify the nomenclature we write

$$\rho_{\mathcal{A}X}(\mathbf{v}) = \rho_X(\mathcal{A}^T \mathbf{v}). \quad (23)$$

C. Acceleration of Parametric Inputs

Let us now consider the following over-approximation for τ on sets:

$$\tau^\sharp(X_0, U) = \mathbf{A}X_0 \oplus \mathbf{B}U \quad (24)$$

Unfolding (3) (ignoring the presence of the guard set G for the time being), we obtain

$$X_n = \mathbf{A}^n X_0 \oplus \sum_{k \in [0, n-1]} \mathbf{A}^k \mathbf{B}U$$

What is left to do is to further simplify the sum $\sum_{k \in [0, n-1]} \mathbf{A}^k \mathbf{B}U$. We can exploit the following simple results from linear algebra.

Lemma 2. *If $\mathbf{I} - \mathbf{A}$ is invertible, then*

$$\sum_{k=0}^{n-1} \mathbf{A}^k = (\mathbf{I} - \mathbf{A}^n)(\mathbf{I} - \mathbf{A})^{-1}$$

. *If furthermore $\lim_{n \rightarrow \infty} \mathbf{A}^n = 0$, then*

$$\lim_{n \rightarrow \infty} \sum_{k=0}^n \mathbf{A}^k = (\mathbf{I} - \mathbf{A})^{-1}$$

This lemma presents a difficulty in the nature of \mathbf{A} . The inverse $(\mathbf{I} - \mathbf{A})^{-1}$, does not exist for eigenvalues of 1, i.e. we need $1 \notin \sigma(\mathbf{A})$, where $\sigma(\mathbf{A})$ is the spectrum (the set of all the eigenvalues) of matrix \mathbf{A} . In order to overcome this problem, we introduce the eigen-decomposition of $\mathbf{A} = \mathbf{J}\mathbf{S}\mathbf{S}^{-1}$, (and trivially $\mathbf{I} = \mathbf{S}\mathbf{I}\mathbf{S}^{-1}$), and by the distributive and transitive properties we obtain

$$(\mathbf{I} - \mathbf{A}^n)(\mathbf{I} - \mathbf{A})^{-1} = \mathbf{S}(\mathbf{I} - \mathbf{J}^n)(\mathbf{I} - \mathbf{J})^{-1}\mathbf{S}^{-1}.$$

This allows us to accelerate the eigenvalues individually, using the property $\sum_{k=0}^{n-1} 1^k = n$ for eigenvalues of $\lambda = 1$. Using the properties above, and translating the problem into the generalised eigenspace to accounting for unit eigenvalues, we obtain the

following representation:

$$\begin{aligned} \sum_{k=0}^{n-1} \lambda^k &= \begin{cases} n & \lambda = 1 \\ \frac{1-\lambda^n}{1-\lambda} & \lambda \neq 1 \end{cases} \\ &\Rightarrow (\mathbf{I} - \mathbf{A}^n)(\mathbf{I} - \mathbf{A})^{-1} = \mathbf{S}\mathbf{D}^n\mathbf{S}^{-1} \\ d(\lambda_i, n, k) &= \frac{-1^k}{k+1} \frac{1-\lambda_i^n}{(1-\lambda_i)^{k+1}} \\ &+ \sum_{j=1}^k \frac{-1^{k-j}}{k-j} \binom{n}{j-1} \frac{\lambda_i^{n-j-1}}{(1-\lambda_i)^{k-j}} \\ \mathbf{D}_{i,j}^n &= \begin{cases} 0 & j < i \\ n & i = j \wedge \lambda_i = 1 \\ \frac{1-\lambda_i^n}{1-\lambda_i} & i = j \wedge \lambda_i \neq 1 \\ 0 & gm(\lambda_i) = 1 \\ \binom{n+1}{k+1} & \lambda_i = 1 \\ d(\lambda_i, n, j-i) & \lambda_i \neq 1 \end{cases} \quad (25) \end{aligned}$$

where $gm(\cdot)$ is the geometric multiplicity of the given eigenvalue.

D. Acceleration of Variable Inputs

The result in the previous section can be only directly applied under restricted conditions in the case of variable inputs. For instance whenever $\forall k > 0, \mathbf{u}_k = \mathbf{u}_{k-1}$. In order to generalise it (in particular to non-constant inputs), we will over-approximate $\mathbf{B}U$ over the eigenspace by a semi-spherical enclosure with centre \mathbf{u}'_c and radius U'_b . To this end, we first rewrite

$$U'_j = \mathbf{S}^{-1}\mathbf{B}U = \{\mathbf{u}'_c\} \oplus U'_d,$$

where \mathbf{u}'_c is the centre of the interval hull of U'_j :

$$\mathbf{u}'_{ci} = \frac{1}{2}(\rho_{U'_j}(\mathbf{v}_i) + \rho_{U'_j}(-\mathbf{v}_i)) \mid \mathbf{v}_{ij} = \begin{cases} 1 & j = i \\ 0 & j \neq i \end{cases}.$$

We then over-approximate U'_d via U'_b , by the maximum radius in the directions of the complex eigenvalues as (cf. illustration in Figure 6). Let

$$\Lambda = \{\lambda_i \mid i \in [1, p], \lambda_i^* \neq \lambda_{i-1}\}$$

$f_b : \mathbb{R}^p \rightarrow \mathbb{R}^{p_b}$ such that

$$f_b(\mathbf{v}) = \text{red}(\mathbf{v}_b) \text{ where } (\mathbf{v}_b)_i = \begin{cases} 0 & \lambda_i \notin \Lambda \\ |\mathbf{v}_i| & \lambda_i \neq \lambda_{i+1}^* \\ \sqrt{\mathbf{v}_i^2 + \mathbf{v}_{i+1}^2} & \lambda_i = \lambda_{i+1}^* \end{cases} \quad \mathcal{L}_b$$

and $\text{red}(\cdot)$ is a function that reduces the dimension of a vector by removing the elements where $\lambda_i \notin \Lambda$.

Extending this to matrices we have

$$F_b : \mathbb{R}^{o \times p} \rightarrow \mathbb{R}^{o \times p_b}$$

$$F_b(\mathbf{C}) = \mathbf{C}_b \text{ where } (\mathbf{C}_b)_{i,*} = f_b(\mathbf{C}_{i,*}) \quad (26)$$

Finally

$$U'_d = \{\mathbf{u} \mid \mathbf{C}'_u \mathbf{u} \leq \mathbf{d}'_u\}$$

$$U'_d \subseteq U'_b = \{\mathbf{u} \mid F_b(\mathbf{C}'_u) f_b(\mathbf{u}) \leq f_b(\mathbf{d}'_u)\}$$

$$\mathbf{B}U \subseteq U_b \oplus U_c \mid U_b = \mathbf{S}U'_b \text{ and } U_c = \{\mathbf{S}\mathbf{u}'_c\} \quad (27)$$

Since the description of U'_b is no longer polyhedral in \mathbb{R}^p , we will also create a semi-spherical over-approximation \mathbf{J}_b of \mathbf{J} in the directions of the complex eigenvectors, in a similar way as we generated U'_b for U'_d . More precisely,

$$\mathbf{J}_b = \begin{bmatrix} \mathbf{J}_{b1} & & \\ & \ddots & \\ & & \mathbf{J}_{br}^n \end{bmatrix} \text{ where} \quad (28)$$

$$\forall s \in [1, r] \left\{ \begin{array}{l} \lambda_j \in \mathbf{J}_{bs} = |\lambda_i| \in \mathbf{J}_s \cap \Lambda \\ gm(\mathbf{J}_{bs}) = gm(\mathbf{J}_s) \end{array} \right.$$

where $gm(\cdot)$ is the geometric multiplicity of the Jordan block.

Definition 1. Given a matrix $\mathbf{A} = \mathbf{S}\mathbf{J}\mathbf{S}^{-1}$ and a vector \mathbf{x} , we define the following operations:

$$F_b^*(\mathbf{A}, \mathbf{x}) = \mathbf{S}f_b^{-1}(F_b(\mathbf{J})f_b(\mathbf{S}^{-1}\mathbf{x})) \quad (29)$$

$$F'_b(\mathbf{A}, \mathbf{x}) = f_b^{-1}(F_b(\mathbf{J})f_b(\mathbf{x}')) \quad (30)$$

Finally, we refer to the accelerated sets

$$U_b^n = \{F_b^*((\mathbf{I} - \mathbf{A}^n), F_b^*((\mathbf{I} - \mathbf{A})^{-1}, \mathbf{u})) \mid \mathbf{u} \in U_b\}$$

$$U_c^n = (\mathbf{I} - \mathbf{A}^n)(\mathbf{I} - \mathbf{A})^{-1}U_c$$

$$U_{cb}^n = U_c^n \oplus U_b^n$$

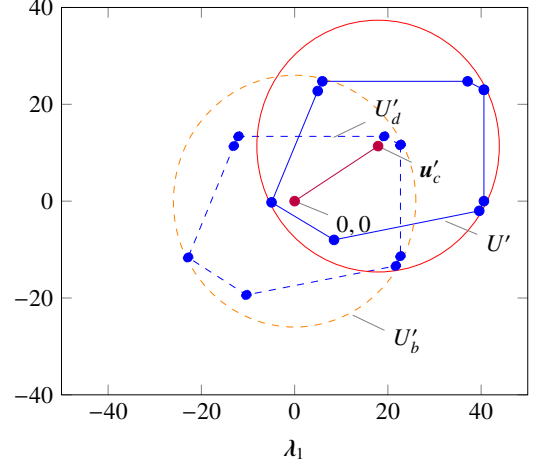


Fig. 6. Relaxation of an input set within a complex subspace, in order to make it invariant to matrix rotations. Dashed lines and curves denote translated quantities onto the origin.

Returning to our original equation for the n -reach set, we obtain²

$$X_n \subseteq \mathbf{A}^n X_0 \oplus U_{cb}^n \quad (31)$$

Shifting our attention from reach sets to tubes, we can now over-approximate the *reach tube* by abstract acceleration of the three summands in (31), as follows.

Theorem 1. *The abstract acceleration*

$$\tau^{\sharp n}(X_0, U) =_{\text{def}} \mathcal{A}^n X_0 \oplus \mathcal{B}^n U_c \oplus \mathcal{B}_b^n U_b \quad (32)$$

is an over-approximation of the n -reach tube, namely $\hat{X}_n \subseteq \tau^{\sharp n}(X_0, U)$.

Proof: The proof is derived from that in [34] for $\mathcal{A}^n X_0$, and extends it as in the developments presented above. ■

E. Combining Abstract Matrices

One important property of the abstract matrices \mathcal{A}^n , \mathcal{B}^n and \mathcal{B}_b^n is that they are correlated. In the

²Note that $\forall U'_b, U'_c, U'_d; \exists U_b, U_c, U_d : U'_b = \mathbf{S}^{-1}BU_b$ so that $U'_c = \mathbf{S}^{-1}BU_c$ and $U'_d = \mathbf{S}^{-1}BU_d$. Hence, this inclusion is also valid in the original state space.

case of parametric inputs, this correlation is linear and described by the acceleration defined in Lemma (2). In the case of \mathcal{B}_b^n this relationship is not linear (see Eq. 27). However, we can still find a linear over-approximation of the correlation between \mathcal{B}_b^n and \mathcal{A}^n based on the time steps k . Given two orthonormal spaces $X \in \mathbb{R}^p \wedge U \in \mathbb{R}^q$ and a transition equation

$$X_{k+1} = \mathbf{A}X_k + \mathbf{B}U,$$

which is related to

$$\rho_{X_{k+1}}(\mathbf{v}) = \rho_{\mathbf{A}X_k}(\mathbf{v}) + \rho_{\mathbf{B}U}(\mathbf{v}),$$

we define a space

$$X' = \left\{ \begin{bmatrix} \mathbf{x} \\ \mathbf{B}\mathbf{u} \end{bmatrix} \mid \mathbf{x} \in X, \mathbf{u} \in U \right\}$$

so that

$$\rho_{X_{k+1}}(\mathbf{v}) = \rho_{X'_k} \begin{bmatrix} \mathbf{A}^T \mathbf{v} \\ \mathbf{v} \end{bmatrix} = \rho_{X'_k}(\mathbf{D}^T \mathbf{v}'),$$

with

$$\mathbf{D} = \begin{bmatrix} \mathbf{A} & 0 \\ 0 & \mathbf{I} \end{bmatrix}, \quad \mathbf{v}' = \begin{bmatrix} \mathbf{v} \\ \mathbf{v} \end{bmatrix}.$$

Accelerating X_{k+1} , we obtain

$$\rho_{X_n}(\mathbf{v}) = \rho_{\mathbf{A}^n X_0}(\mathbf{v}) + \rho_{(\mathbf{I} - \mathbf{A}^n)(\mathbf{I} - \mathbf{A})^{-1} \mathbf{B}U}(\mathbf{v}) = \rho_{X'_0}(\mathbf{D}^{nT} \mathbf{v}'),$$

with

$$\mathbf{D}^n = \begin{bmatrix} \mathbf{A}^n & 0 \\ 0 & (\mathbf{I} - \mathbf{A}^n)(\mathbf{I} - \mathbf{A})^{-1} \end{bmatrix}$$

in the case of parametric inputs. More generally, the diagonal elements of \mathbf{D}^n correspond to the diagonal elements of \mathbf{A}^n and $\sum_{k=0}^{n-1} \mathbf{A}^k \mathbf{B}$, which means we can construct

$$\mathcal{D}^n = \begin{bmatrix} \mathcal{A}^n & 0 \\ 0 & \mathcal{B}^n \end{bmatrix} \mid \rho_{X_n}(\mathbf{v}) = \rho_{X'_0}(\mathcal{D}^{nT} \mathbf{v}'). \quad (33)$$

We can then apply this abstraction to (27) and obtain:

$$\rho_{X_n}(\mathbf{v}) = \rho_{X'_0}(\mathcal{D}^{nT} \mathbf{v}') \text{ where} \quad (34)$$

$$\begin{aligned} \mathcal{D}_b^n &= \begin{bmatrix} \mathcal{A}^n & 0 \\ 0 & \mathcal{B}_b^n \end{bmatrix}, \quad \mathbf{v}' = \begin{bmatrix} \mathbf{v} \\ f_b(\mathbf{v}) \end{bmatrix} \\ \mathcal{B}_b^n &= \mathbf{S} \mathbf{F}_b^{-1} \left((\mathbf{I} - \mathcal{J}_b^n)(\mathbf{I} - \mathbf{J}_b)^{-1} \mathbf{F}_b(\mathbf{S}^{-1}) \right) \end{aligned}$$

with \mathbf{J}_b defined by (28). This model provides a tighter over-approximation than (32) since the accelerated dynamics of the inputs are now constrained by the accelerated dynamics of the system.

VI. ABSTRACT ACCELERATION WITH GUARDS: ESTIMATION OF THE NUMBER OF ITERATIONS

The most important task remaining is how to calculate the number of iterations dealing with the presence of the guard set G .

Given a convex polyhedral guard expressed as the assertion $\{\mathbf{x} \mid \mathbf{G}\mathbf{x} \leq \mathbf{h}\}$, we define $G_{i,*}$ as the i^{th} row of \mathbf{G} and h_i as the corresponding element of \mathbf{h} . We denote the normal vector to the i^{th} face of the guard as $\mathbf{g}_i = G_i^T$. The distance of the guard to the origin is thus $\gamma_i = \frac{h_i}{\|\mathbf{g}_i\|}$.

Given a convex set X , we may now describe its position with respect to each face of the guard through the use of its support function alongside the normal vector of the hyperplane (for clarity, we assume the origin to be inside set X):

$$\begin{aligned} \rho_X(\mathbf{g}_i) &\leq \gamma_i, & \text{inside the hyperplane,} \\ -\rho_X(-\mathbf{g}_i) &\geq \gamma_i, & \text{outside the hyperplane.} \end{aligned}$$

Applying this to equation (31) we obtain:

$$\rho_{X_n}(\mathbf{g}_i) = \rho_{X_0}(\mathbf{A}^{n_i T} \mathbf{g}_i) + \rho_{U_{cb}^n}(\mathbf{g}_i) \leq \gamma_i \quad (35)$$

$$\rho_{X_n}(-\mathbf{g}_i) = \rho_{X_0}(-\mathbf{A}^{\bar{n}_i T} \mathbf{g}_i) + \rho_{U_{cb}^n}(-\mathbf{g}_i) \leq -\gamma_i \quad (36)$$

From the inequalities above we can determine up to which number of iterations \underline{n}_i the reach tube remains inside the corresponding hyperplane, and starting from which iteration \bar{n}_i the corresponding reach set goes beyond the guard:

In order for a reach set to be inside the guard it must therefore be inside all of its faces, and we can ensure it is fully outside of the guard set when it is fully beyond any of them. Thus, we have $\underline{n} = \min\{ \underline{n}_i \}$, and $\bar{n} = \min\{ \bar{n}_i \}$.

We have not however discussed why these two cases are important. Looking at the transition in equation (1), we can easily derive that if $\mathbf{G}\mathbf{x}_k \not\leq \mathbf{h}$

the postimage of all subsequent iterations is empty. Therefore, any overapproximation henceforth will only add imprecision. We will use the bounds \underline{n} and \bar{n} to create a tighter overapproximation. Let

$$\begin{aligned}\hat{X}_{\underline{n}}^\# &= \mathcal{A}_{\underline{n}}X_0 \oplus \mathcal{B}_{\underline{n}}U && \text{(n-reachtube)} \\ X_{\underline{n}}^\# &= A_{\underline{n}}X_0 \oplus \mathcal{B}_{\underline{n}}U && \text{(n-reachset)} \\ \hat{X}_{\bar{n} | \underline{n}}^\# &= \tau(\mathcal{A}_{\bar{n}-\underline{n}-1}X_{\underline{n}}^\# \oplus \mathcal{B}_{\underline{n}}U \cap G, U) \\ \hat{X}_{\bar{n}}^\# &= \hat{X}_{\bar{n} | \underline{n}}^\# \cup \hat{X}_{\underline{n}}^\#\end{aligned}\quad (37)$$

This double step prevents the set $\{\mathbf{x} \mid \mathbf{x} \in \hat{X}_{\underline{n}}^\#, \mathbf{x} \notin X_{\underline{n}}^\#\}$ to be included in further projections, thus reducing the size of the overapproximation.

Computing the maximum \underline{n}_i such that (35) is satisfied is not easy because the unknown \underline{n}_i occurs in the exponent of the equation. However, since an intersection with the guard set will always return a sound over-approximation, we do not need a precise value. We can over-approximate it by decomposing \mathbf{g}_i into the generalised eigenspace of \mathbf{A} . Let $\mathbf{g}_i = \sum_{j=1}^p k_{ij}\mathbf{v}_j + \text{res}(\mathbf{g}_i)$, where \mathbf{v}_j are row vectors of \mathbf{S}^{-1} or $-\mathbf{S}^{-1}$ such that $k_{ij} \geq 0$, and $\text{res}(\mathbf{g}_i)$ is the component of \mathbf{g}_i that lies outside the range of \mathbf{S} . Notice that since \mathbf{S} has an inverse, it is full rank and therefore $\text{res}(\mathbf{g}_i) = \mathbf{0}$ and subsequently not relevant. It is also important to note that \mathbf{S} is the matrix of generalised eigenvectors of \mathbf{A} and therefore we are expressing our guard in the generalised eigenspace of \mathbf{A} .

$$\rho_{X_0}(\mathbf{A}^{nT} \mathbf{g}_i) = \rho_{X_0} \left(\sum_{j=1}^p k_{ij} \mathbf{A}^{nT} \mathbf{v}_j \right) \leq \sum_{j=1}^p k_{ij} \rho_{X_0}(\mathbf{A}^{nT} \mathbf{v}_j) \quad (38)$$

A. Overestimating the Iterations of a loop without inputs

We start by looking into the approximation of the inside bound (i.e. the iterations for which the reachtube remains fully inside the guard). Since rotating dynamics and Jordan shapes will have a complex effect on the behaviour of the equation, we seek to transform the Jordan form into a real positive

diagonal. In such a case, the progression of the support function in each direction is monotonically increasing (or decreasing) and it is therefore very easy to find a bound for its progression. We note that the envelope of rotating dynamics will always contain the true dynamics and is therefore a sound overapproximation. We will initially assume that γ_i is positive and then extend to the general case.

Let $\rho_{X_0}(\mathbf{A}^{nT} \mathbf{g}_i) = \rho_{X'_0}(\mathbf{J}^{nT} \mathbf{g}'_i)$ such that

$$\begin{aligned}\mathbf{g}'_i &= \mathbf{S}^{-1} \mathbf{g}_i \\ X_0 &= \{\mathbf{x} \mid \mathbf{C}_{X_0} \mathbf{x} \leq \mathbf{d}_{X_0}\} \\ X'_0 &= \mathbf{S}^{-1} X_0 = \{\mathbf{x} \mid \mathbf{S} \mathbf{C}_{X_0} \mathbf{x} \leq \mathbf{d}_{X_0}\}\end{aligned}$$

Let

$$\Lambda_\sigma = \{\lambda_i : i \in [1, p], \bigwedge_{j=1}^{i-1} (\lambda_i^* \neq \lambda_j \wedge \lambda_i \neq \lambda_j)\}$$

$$f_\sigma(\mathbf{v}) : \mathbb{R}^p \rightarrow \mathbb{R}^{p_b}$$

$$f_\sigma(\mathbf{v}) = \text{red}(\mathbf{v}_\sigma)$$

$$\text{where } (\mathbf{v}_\sigma)_i = \begin{cases} 0 & \lambda_i \notin \Lambda_\sigma \\ \sqrt{\sum_{j \in [1, p] \wedge (\lambda_j = \lambda_i \vee \lambda_j = \lambda_i^*)} \mathbf{v}_j^2} & \lambda_i \in \Lambda_\sigma \end{cases}$$

$$F_\sigma : \mathbb{R}^{o \times p} \rightarrow \mathbb{R}^{o \times r}$$

$$F_\sigma(\mathbf{C}) = \mathbf{C}_\sigma \text{ where } (\mathbf{C}_\sigma)_{i,*} = f_\sigma(\mathbf{C}_{i,*}).$$

and $\text{red}(\cdot)$ is a function that reduces the dimension of a vector by removing the elements where $\lambda_i \notin \Lambda_\sigma$. This reduction is not strictly necessary, but it enables a faster implementation by reducing dimensionality. Correspondingly, given $\mathbf{J} = \text{diag}(\{\mathbf{J}_s \mid s \in [1, r]\})$

$$\mathbf{J}_\sigma = \begin{bmatrix} \bar{\sigma}_1 & 0 & \cdots & 0 \\ 0 & \bar{\sigma}_2 & \cdots & 0 \\ 0 & 0 & \ddots & 0 \\ 0 & 0 & \cdots & \bar{\sigma}_r \end{bmatrix} \quad (39)$$

where $\bar{\sigma}_s = \|\mathbf{J}_s\|_2$ is the maximum singular value (hence the induced norm [36]) of the Jordan block \mathbf{J}_s .

Finally, let

$$\mathbf{x}'_c = \frac{1}{2}(\rho_{X'_0}(\mathbf{v}_i) + \rho_{X'_0}(-\mathbf{v}_i)), \quad \mathbf{v}_{ij} = \begin{cases} 1 & j = i \\ 0 & j \neq i \end{cases}$$

$$X'_\sigma = \{\mathbf{x} \mid F_\sigma(\mathbf{S}C_{X_0})f_\sigma(\mathbf{x}) \leq f_\sigma(\mathbf{d}_{X_0} - \mathbf{S}C_{X_0}\mathbf{x}'_c)\}$$

$$X'_0 \subseteq f_\sigma^{-1}(X'_{c\sigma}) \mid X'_{c\sigma} = \{f_\sigma(\mathbf{x}'_c)\} \oplus X'_\sigma \quad (40)$$

and $\mathbf{v}_\sigma = f_\sigma(\mathbf{v})$.

Using eigenvalue and singular value properties, we obtain $\rho_{X_0}(\mathbf{A}^{nT}\mathbf{v}_j) \leq \bar{\sigma}_j^n \rho_{X_{c\sigma}}((\mathbf{v}_\sigma)_j) \mid j \in [1, r]$, and therefore:

$$\rho_{X_0}(\mathbf{A}^{nT}\mathbf{g}_i) \leq \sum_{j=1}^p k_{ij} \bar{\sigma}_j^n \rho_{X_{c\sigma}}((\mathbf{v}_\sigma)_j) \quad (41)$$

Since we have no inputs, $\rho_{U_c}(\mathbf{g}_i) + \rho_{U_b}(\mathbf{g}_i) = 0$, hence we may solve for \underline{n}_i :

$$\rho_{X_0}(\mathbf{A}^{nT}\mathbf{g}_i) \leq \sum_{j=1}^p k_{ij} \bar{\sigma}_j^{\underline{n}_i} \rho_{X_{c\sigma}}((\mathbf{v}_\sigma)_j) \leq \gamma_i \quad (42)$$

To separate the divergent element of the dynamics from the convergent one, let us define

$$\bar{k}_{ij} = \max(k_{ij} \rho_{X_{c\sigma}}((\mathbf{v}_\sigma)_j), 0)$$

$$\bar{\sigma} = \max(\{\bar{\sigma}_s \mid s \in [1, p]\}).$$

This step will allow us to track effectively which trajectories are likely to hit the guard and when, since it is only the divergent element of the dynamics that can increase the reach tube in a given direction.

Replacing (42), we obtain

$$\bar{\sigma}^n \sum_{j=1}^p \bar{k}_{ij} \left(\frac{\bar{\sigma}_j}{\bar{\sigma}}\right)^n \leq \gamma_i, \quad (43)$$

which allows to finally formulate an iteration scheme for approximating n .

Proposition 1. *An iterative under-approximation of the number of iterations n can be computed by starting with $\underline{n}_i = 0$ and iterating over*

$$\underline{n}_i \geq n = \log_{\bar{\sigma}}(\gamma_i) - \log_{\bar{\sigma}}\left(\sum_{j=1}^p \bar{k}_{ij} \left(\frac{\bar{\sigma}_j}{\bar{\sigma}}\right)^{\underline{n}_i}\right), \quad (44)$$

substituting $n_i = n$ on the right-hand side until we meet the inequality.

Proof: This follows from the developments unfolded above. Notice that the sequence \underline{n}_i is monotonically increasing, before it breaks the inequality. As such any local minimum represents a sound under-approximation of the number of loop iterations. Note that in the case where $\gamma_i \leq 0$ we must first translate the system coordinates such that $\gamma_i > 0$. This is simply done by replacing $\mathbf{x}' = \mathbf{x} + \mathbf{c}$ and operating over the resulting system where $\gamma'_i = \rho_c(\mathbf{g}_i) + \gamma_i$.

Mathematically this is achieved as follows: first we get \mathbf{c} by finding the center of the interval hull of G (if G is open in a given direction we may pick any number in that direction for the corresponding row of c). Next we transform the dynamics into

$$\begin{bmatrix} \mathbf{x}_k \\ \mathbf{1} \end{bmatrix} = \begin{bmatrix} \mathbf{A} & \mathbf{A}\mathbf{c} \\ \mathbf{0} & \mathbf{1} \end{bmatrix} \begin{bmatrix} \mathbf{x}_{k-1} \\ \mathbf{1} \end{bmatrix} + \begin{bmatrix} \mathbf{B} \\ \mathbf{0} \end{bmatrix} \mathbf{u}_k \mid \begin{bmatrix} \mathbf{x}_{k-1} \\ \mathbf{1} \end{bmatrix} \in G'$$

where

$$G' = \left\{ \begin{bmatrix} \mathbf{x} \\ \mathbf{1} \end{bmatrix} \mid \begin{bmatrix} \mathbf{G} & \mathbf{G}\mathbf{c} \\ \mathbf{0} & \mathbf{1} \end{bmatrix} \begin{bmatrix} \mathbf{x}_{k-1} \\ \mathbf{1} \end{bmatrix} \leq \begin{bmatrix} \mathbf{h} \\ \mathbf{1} \end{bmatrix} \right\}$$

■

B. Underestimating the Iterations of a loop without inputs

In order to apply a similar techniques to (36) we must find an equivalent under-approximation. In the case of equation (42), the $\bar{\sigma}_j$ ensure that the equation diverges faster than the real dynamics, hence the iteration found is an upper bound to the desired iteration. In this case we want the opposite, hence we look for a model where the dynamics diverge slower. In this case it is easy to demonstrate that $\lambda_{b_j} = |\lambda_j|$ represents these slower dynamics.

$$\rho_{X_0}(-\mathbf{A}^{\bar{n}_i T}\mathbf{g}_i) \leq \sum_{j=1}^p k_{ij} \lambda_{b_j}^{\bar{n}_i} \bar{k}_{ij} \rho_{X_{c\sigma}}(-(\mathbf{v}_\sigma)_j) \leq -\gamma_i \quad (45)$$

which reduces to

$$\bar{\sigma}^n \sum_{j=1}^p \bar{k}_{ij}^- \left(\frac{\lambda_{b_j}}{\bar{\sigma}}\right)^n + \bar{\sigma}^n \sum_{j=1}^p \bar{k}_{ij}^+ \leq -\gamma_i, \quad (46)$$

where

$$\begin{aligned} \underline{k}_{ij}^- &= \min(k_{ij} \rho_{X_{cr}}(-\mathbf{v}_\sigma)_j, 0) \\ \underline{k}_{ij}^+ &= \max(k_{ij} \rho_{X_{cr}}(-\mathbf{v}_\sigma)_j, 0) \end{aligned}$$

An additional consideration must also be made regarding the rotational nature of the dynamics. In the previous case we did not care about the rotational alignment of the set X_n with respect to the vector \mathbf{g}_i , because any rotation would move the set inside the guard. In this case, although the magnitude of the resulting vector is greater than the required one, the rotation may cause it to be at an angle that keeps the set inside the guard. We must therefore account for the rotating dynamics in order to find the point where the angles align with the guard. In order to do this, let us first fix the magnitudes of the powered eigenvalues, in the case of convergent dynamics we will assume they have converged a full rotation in to make our equation strictly divergent. Let $\underline{\theta} = \min\{\theta_j \mid j \in [1, p]\}$, where θ_j are the angles of the complex conjugate eigenvalues. Let $n_\theta = \frac{2\pi}{\underline{\theta}}$ be the maximum number of iterations needed for any of the dynamics to complete a full turn. Then at any given turn $|\lambda_j|^{\bar{n}_i + n_\theta} \leq |\lambda_j|^{\bar{n}_i + n} \mid |\lambda_j| \leq 1, n \in 0n_\theta$. This means that any bound we find on the iterations will be necessarily smaller than the true value. Our problem becomes the solution to:

$$\begin{aligned} &\max \left(\bar{\sigma}^{\bar{n}_i} \sum_{j=1}^p c_{ij} \cos((n - \bar{n}_i)\theta_j - \alpha_{ij}) \right) \\ a_{ij} &= \cos^{-1}(\mathbf{g}_i \cdot \mathbf{v}_j) \\ c_{ij} &= \begin{cases} \underline{k}_{ij}^- \left(\frac{\lambda_{bj}}{\bar{\sigma}} \right)^{\bar{n}_i} & |\lambda_j| \geq 1 \\ \underline{k}_{ij}^- \left(\frac{\lambda_{bj}}{\bar{\sigma}} \right)^{\bar{n}_i + n_\theta} & |\lambda_j| < 1 \end{cases} \end{aligned}$$

The problem is simplified by underapproximating the

cosines and removing the constants:

$$\begin{aligned} &\max \left(\bar{\sigma}^{\bar{n}_i} \sum_{j=1}^p c_{ij} \left(1 - \frac{((n - \bar{n}_i)\theta_j - \alpha_{ij})^2}{2} \right) \right) \\ \Rightarrow &\min \left(\sum_{j=1}^p c_{ij} ((n - \bar{n}_i)\theta_j - \alpha_{ij})^2 \right) \\ \Rightarrow &\min \left(\sum_{j=1}^p c_{ij} \theta_j^2 (n - \bar{n}_i)^2 + c_{ij} \alpha_{ij} \theta_j (n - \bar{n}_i) \right) \end{aligned}$$

The solution to this equation is

$$n = \bar{n}_i - \frac{\sum_{j=1}^p c_{ij} \alpha_{ij} \theta_j}{2 \sum_{j=1}^p c_{ij} \theta_j^2} \mid n \in [\bar{n}_i, \bar{n}_i + n_\theta] \quad (47)$$

The second part of the equation is expected to be a positive value. When this is not the case, the dominating dynamics will have a rotation $\theta_j \geq \frac{\pi}{2}$. In such cases we must explicitly evaluate the set of up to 4 iterations after \bar{n}_i . If the resulting bound does not satisfy the original inequality: $\rho_{X_0}(\mathbf{A}^{\bar{n}_i T} \mathbf{g}_i) \geq \gamma_i$, we replace $\bar{n}_i = n$ until it does³.

Proposition 2. *An iterative under-approximation of the number of iterations n can be computed by starting with $\bar{n}_i' = 0$ and iterating over*

$$\begin{aligned} \bar{n}_i' &\leq n = \log_{\bar{\sigma}}(\gamma_i) - \log_{\bar{\sigma}} \left(\sum_{j=1}^p \underline{k}_{ij}^- \left(\frac{\lambda_{bj}}{\bar{\sigma}} \right)^{\bar{n}_i'} + \sum_{j=1}^p \underline{k}_{ij}^+ \right) \\ \bar{n}_i &= \bar{n}_i' + k \mid \rho_{X_0}(\mathbf{A}^{(\bar{n}_i' + k) T} \mathbf{g}_i) \geq \gamma_i \end{aligned} \quad (48)$$

where k is the result of equation (47). we substitute for $\bar{n}_i = n$ on the right-hand side until we break the inequality, and then find k such that the second inequality holds.

Since we are explicitly verifying the inequality, there is no further proof required.

C. Estimating the Iterations of a loop with inputs

For the case with inputs, we will use the same paradigm explained in the previous section after performing a mutation that transforms the system with

³this is a tighter value than work shown on previous versions of this paper where we overapproximated using $n_\theta = \frac{(2\pi)^m}{\prod_j \theta_j}$, where m is the number of conjugate pairs.

inputs into an over-approximating system without inputs.

Let $X'_{c\sigma}, U'_{c\sigma}$ be the corresponding sets of initial states and inputs obtained by applying equation (40) to X'_0 and U'_j , and let $U'_{J\sigma} = (\mathbf{I} - \mathbf{J}_\sigma)^{-1}U'_{c\sigma}$. The accelerated resulting system may be represented by the equations

$$\begin{aligned} (X'_{c\sigma})_n &= \mathbf{J}'_\sigma X'_{c\sigma} \oplus (\mathbf{I} - \mathbf{J}'_\sigma)U'_{J\sigma} \\ \rho_{(X'_{c\sigma})_n}(\mathbf{v}) &= \rho_{X'_{c\sigma}}(\mathbf{J}'_\sigma \mathbf{v}) + \rho_{U'_{J\sigma}}(\mathbf{v}) - \rho_{U'_{J\sigma}}(\mathbf{J}'_\sigma \mathbf{v}) \end{aligned} \quad (49)$$

Let us now define $(XU)_\sigma = \{\mathbf{x} - \mathbf{u} \mid \mathbf{x} \in X'_{c\sigma}, \mathbf{u} \in U'_{J\sigma}\}$ which allows us to translate the system into

$$\rho_{((XU)_\sigma)_n}(\mathbf{v}) = \rho_{(XU)_\sigma}(\mathbf{J}'_\sigma \mathbf{v}) \quad (50)$$

which has the same shape as the equations in the previous section. We may now apply the techniques described above to find the bounds on the iterations.

D. Narrowing the estimation of the iterations

The estimations above are very conservative, but we may use further techniques to obtain tighter bounds on the number of iterations. In the first instance we note that we have eliminated all negative terms in the sums in equation (44). Reinstating these terms can cause us to lose monotonicity, but we may still create an iterative approach by fixing the negative value at intermediate stages. Let \underline{n}_i be our existing bound for the time horizon before reaching a guard, and $\underline{k}_{n_i} = \sum_{j=1}^p k_{ij} \left(\frac{\bar{\sigma}_j}{\underline{\sigma}}\right)^{\underline{n}_i}$, $\bar{k}_{n_i} = \sum_{j=1}^p \bar{k}_{ij} \left(\frac{\bar{\sigma}_j}{\underline{\sigma}}\right)^{\underline{n}_i}$ the corresponding negative and positive terms of the equation. We may now find upper and lower bounds for \underline{n}_i by replacing the equation

$$\underline{n}_i \geq n_k = \log_{\underline{\sigma}}(\gamma_i) - \log_{\underline{\sigma}}(\bar{k}_{n_i} + \underline{k}_{n_i}) \quad (51)$$

where \underline{n}_k is the bound found in the previous stage. Some stages of this process will provide an unsound result, but they will also provide an upper bound to our number of iterations. In fact, every second stage will provide a monotonically increasing sound bound which will be tighter than the one in equation (44).

Proof: Since the elements of the sums are convergent, we have

$$\begin{aligned} n_i \geq n_k &\Rightarrow \underline{k}_{n_i} \geq \underline{k}_{n_k} \text{ (i.e. } |\underline{k}_{n_i}| \leq |\underline{k}_{n_k}|) \\ &\Rightarrow \log_{\underline{\sigma}}(\bar{k}_{n_i} + \underline{k}_{n_i}) \geq \log_{\underline{\sigma}}(\bar{k}_{n_k} + \underline{k}_{n_k}) \end{aligned}$$

which means that n_k in equation (51) is smaller than or n in equation (44) ($n_k \leq n \leq \underline{n}_i \mid \underline{n}_i \geq \underline{n}_k$). ■

In the case of equation (48), the explicit evaluation of the guard at each cycle executes the behaviour described here.

E. Maintaining Geometric Multiplicity

A second step in optimising the number of iterations comes from adding granularity to the bounding semi-spherical abstraction by retaining the geometric multiplicity using the matrix \mathbf{J}_b .

Lemma 3. *Given a matrix \mathbf{A} with eigenvalues $\{\lambda_s \mid s \in [1, r]\}$, where each eigenvalue λ_s has a geometric multiplicity p_s and corresponding generalised eigenvectors $\{\mathbf{v}_{s,i} \mid i \in [1, p_s]\}$,*

$$\begin{aligned} \forall n \geq 0, \mathbf{A}^n \mathbf{v}'_s &= \lambda_s^n \mathbf{v}_{s,i} + \sum_{j=1}^{i-1} \lambda_s^{n-j} \prod_{k=0}^{j-1} (n-k) \mathbf{v}_{s,i-j} \\ &= \lambda_s^n \left(\mathbf{v}_{s,i} + \sum_{j=1}^{i-1} \frac{\prod_{k=0}^{j-1} (n-k)}{\lambda_s^j} \mathbf{v}_{s,i-j} \right) \end{aligned} \quad (52)$$

Proof: By definition, given an eigenvector \mathbf{v}_s of \mathbf{A} , then $\mathbf{A}\mathbf{v}_s = \lambda_s \mathbf{v}_s$ [32]. Similarly a generalised eigenvector $\mathbf{v}_{s,i}$ of \mathbf{A} satisfies the equation $(\mathbf{A} - \lambda_s \mathbf{I})\mathbf{v}_{s,i} = \mathbf{v}_{s,i-1}$ and $\mathbf{v}_{s,1} = \mathbf{v}_s$ hence

$$\begin{aligned} \mathbf{A}\mathbf{v}_{s,i} &= \lambda_s \mathbf{v}_{s,i} + \mathbf{v}_{s,i-1} \\ \mathbf{A}^n \mathbf{v}_{s,1} &= \lambda_s^n \mathbf{v}_{s,1} \\ \mathbf{A}^n \mathbf{v}_{s,i} &= \mathbf{A}^{n-1}(\lambda_s \mathbf{v}_{s,i} + \mathbf{v}_{s,i-1}) = \lambda_s \mathbf{A}^{n-1} \mathbf{v}_{s,i} + \mathbf{A}^{n-1} \mathbf{v}_{s,i-1} \\ &= \lambda_s^2 \mathbf{A}^{n-2} \mathbf{v}_{s,i} + \lambda_s \mathbf{A}^{n-2} \mathbf{v}_{s,i-1} + \mathbf{A}^{n-1} \mathbf{v}_{s,i-1} \\ &= \dots = \lambda_s^n \mathbf{v}_{s,i} + \sum_{j=0}^{n-1} \lambda_s^j \mathbf{A}^{n-j-1} \mathbf{v}_{s,i-1} \end{aligned}$$

From here we recursively expand the formula for $\mathbf{A}^{n-j-1}\mathbf{v}_{s,i-1}$ and obtain:

$$\begin{aligned}\mathbf{A}^n\mathbf{v}_{s,i} &= \lambda_s^n\mathbf{v}_{s,i} + \sum_{j=0}^{n-1}\lambda_s^j\lambda_s^{n-j-1}\mathbf{v}_{s,i-1} + \sum_{j=0}^{n-1}\sum_{k=0}^{n-2}\lambda_s^k\mathbf{A}^{n-k-2}\mathbf{v}_{s,i-2} \\ &= \lambda_s^n\mathbf{v}_{s,i} + n\lambda_s^{n-1}\mathbf{v}_{s,i-1} + n\sum_{j=0}^{n-2}\lambda_s^j\mathbf{A}^{n-j-2}\mathbf{v}_{s,i-2} \\ &= \dots = \lambda_s^n\mathbf{v}_{s,i} + \sum_{j=1}^{i-1}\lambda_s^{n-j}\prod_{k=0}^{j-1}(n-k)\mathbf{v}_{s,i-j}\end{aligned}$$

Let i' denote the position of $f_b(\lambda_j)$ within the block \mathbf{J}_{bs} it belongs to, such that its corresponding generalised eigenvector is identified as $\mathbf{v}_{bs,i'} = f_b(\mathbf{v}_j)$. Then

$$\begin{aligned}\rho_{X_0}(\mathbf{J}^{nT}\mathbf{g}'_i) &\leq \sum_{j=1}^{p_b} k_{ij}\rho_{X_0}(\mathbf{J}_b^{nT}f_b(\mathbf{v}_j)) \\ &\leq \sum_{j=1}^{p_b} k_{ij}\lambda_{b_j}^n\rho_{X_0}\left(\mathbf{v}_{bs,i'} + \sum_{k=1}^{i'-1}\frac{\prod_{m=0}^{k-1}(n-m)}{\lambda_{b_j}^k}\mathbf{v}_{bs,i'-k}\right) \\ &\leq \sum_{j=1}^{p_b} k_{ij}\lambda_{b_j}^n\left(\rho_{X_0}(\mathbf{v}_{bs,i'}) + \sum_{k=1}^{i'-1}\frac{\prod_{m=0}^{k-1}(n-m)}{\lambda_{b_j}^k}\rho_{X_0}(\mathbf{v}_{bs,i'-k})\right) \\ &\leq \sum_{j=1}^{p_b} k'_{ij_0}\lambda_{b_j}^n + \sum_{m=1}^{i'} k'_{ij_m}\lambda_{b_j}^n \prod_{m=0}^{p_s-i'-1} (n-m)\end{aligned}\quad (53)$$

In order to manage the product on the right hand side we use slightly different techniques for over- and under-approximations. For \underline{n}_i we first find an upper bound \underline{n}'_i using equation (44) and $k_{ij} = k'_{ij_0} + k'_{ij_m}$ and then do a second iteration using $k_{ij} = k'_{ij_0} + k'_{ij_m} \prod_{m=0}^{p_s-i'-1} (\underline{n}'_i - m)$ which ensures the true value is under the approximation. In the case of \bar{n}_i , we also start with $k_{ij} = k'_{ij_0} + k'_{ij_m}$ and update it during the iterative process.

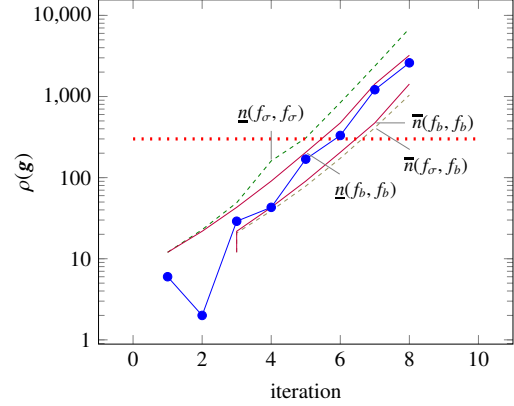


Fig. 7. Progression of the support function of a system for a given guard. Blue dots are real values. The dashed green line overapproximates the progression using singular values (sec VI-A), the dashed yellow line underapproximates them using eigenvalue norms (sec VI-B), whereas the continuous purple lines represent the tighter overapproximation maintaining the gemoetric multiplicity (sec VI-E). We can see how the purple line finds a better bound for \underline{n}_i , while the \bar{n}_i bound is conservative for both approaches. Mind the logarithmic scale.

Let us look at the following example:

$$\mathbf{J} = \begin{bmatrix} 3 & 0 & 0 & 0 & 0 & 0 \\ 0 & 2 & 1 & 0 & 0 & 0 \\ 0 & 0 & 2 & 0 & 0 & 0 \\ 0 & 0 & 0 & -2 & 0 & 0 \\ 0 & 0 & 0 & 0 & -1 & 1 \\ 0 & 0 & 0 & 0 & -1 & -1 \end{bmatrix}$$

$$\mathbf{S} = \begin{bmatrix} 1 & 0 & 0 & 0 & 0 & 0 \\ 0 & 3 & 0 & 0 & 0 & 0 \\ 0 & -4 & 1 & 0 & 0 & 0 \\ 0 & 0 & 0 & 1 & 0 & 0 \\ 0 & 0 & 0 & 0 & 1 & 0 \\ 0 & 0 & 0 & 0 & 1 & 1 \end{bmatrix}$$

$$\mathbf{J}_\sigma = \begin{bmatrix} 3 & 0 & 0 & 0 \\ 0 & 3 & 0 & 0 \\ 0 & 0 & 2 & 0 \\ 0 & 0 & 0 & \sqrt{2} \end{bmatrix}$$

$$\mathbf{x}'_0 = [1 \ 1 \ 1 \ 1 \ 1 \ 1]$$

$$\mathbf{G}\mathbf{x} \leq 300 \mid \mathbf{G} = [1 \ 3 \ -3 \ 2 \ 4 \ 1]$$

$$\mathbf{G} = [1 \ 1 \ 1 \ 2 \ 4 \ -3] \mathbf{S}^T$$

The progression of the system along the support function and corresponding bounds as described in the previous section are shown in figure 7

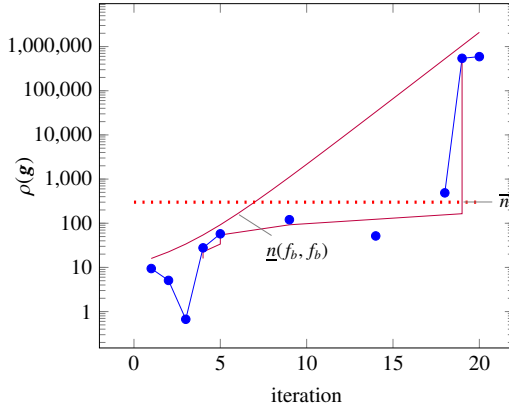


Fig. 8. Progression of the support function of a rotational system for a given guard. Blue dots are real values (negative values are missing due to the log scale). Continuous purple lines represent the overapproximation. The steep vertical line at 19 is due to the alignment of the rotations with the guard at this point. The point at iteration 14 appears below the line because of the higher point at iteration 9. The model will either find that this boundary was met at iteration 9 or push it forward to 19.

Changing the eigenvalues to:

$$J = \begin{bmatrix} 2e^{-0.2i} & 0 & 0 & 0 & 0 & 0 \\ 0 & 2e^{0.2i} & 0 & 0 & 0 & 0 \\ 0 & 0 & \sqrt{2}e^{-0.3i} & 0 & 0 & 0 \\ 0 & 0 & 0 & \sqrt{2}e^{0.3i} & 0 & 0 \\ 0 & 0 & 0 & 0 & 1.1e^{0.5i} & 0 \\ 0 & 0 & 0 & 0 & 0 & 1.1e^{-0.5i} \end{bmatrix}$$

we get the results in figure 8. In this case we can see that the rotational dynamics force an increase of the initially calculated iteration to account for the effects of the rotation.

F. Case Study

We have selected a known benchmark to illustrate the discussed procedure: the room temperature control problem [17]. The temperature (variable `temp`) of a room is controlled to a user-defined set point (`set`), which can be changed at any time through a heating (`heat`) element, and is affected by ambient temperature (`amb`) that is out of the control of the system.

We formalise the description of such a system both via a linear loop and via hybrid dynamics. Observe that since such a system may be software controlled,

we assume that part of the system is coded, and further assume that it is possible to discretise the physical environment for simulation. Algorithm 1 shows a pseudo-code fragment for the temperature control problem. We use the `read` function to

Algorithm 1 Temperature Control Loop

States: `temp`=temperature, `heat`=heat output.

Inputs: `set`=set-point, `amb`=ambient temperature.

```

1: temp=5+read(35);
2: heat=read(1);
3: while(temp< 400 && heat< 300)
4: {
5:   amb=5+read(35);
6:   set=read(300);
7:   temp=.97 temp + .02 amb + .1 heat;
8:   heat=heat + .05 set;
9: }
```

represent non-deterministic values between 0 and the maximum given as argument. Alternatively, this loop corresponds to the following hybrid dynamical model:

$$\begin{bmatrix} \text{temp} \\ \text{heat} \end{bmatrix}_{k+1} = \begin{bmatrix} 0.97 & 0.1 \\ -0.05 & 1 \end{bmatrix} \begin{bmatrix} \text{temp} \\ \text{heat} \end{bmatrix}_k + \begin{bmatrix} 0.02 & 0 \\ 0 & 0.05 \end{bmatrix} \begin{bmatrix} \text{amb} \\ \text{set} \end{bmatrix}_k,$$

with initial condition

$$\begin{bmatrix} \text{temp} \\ \text{heat} \end{bmatrix}_0 \in \begin{bmatrix} [5 \ 40] \\ [0 \ 1] \end{bmatrix},$$

non-deterministic inputs

$$\begin{bmatrix} \text{amb} \\ \text{set} \end{bmatrix}_k \in \begin{bmatrix} [5 \ 40] \\ [0 \ 300] \end{bmatrix},$$

and guard set

$$G = \left\{ \left[\begin{bmatrix} \text{temp} \\ \text{heat} \end{bmatrix} \mid \begin{bmatrix} 1 & 0 \\ 0 & 1 \end{bmatrix} \begin{bmatrix} \text{temp} \\ \text{heat} \end{bmatrix} < \begin{bmatrix} 400 \\ 300 \end{bmatrix} \right\}.$$

In this model the variables are continuous and take values over the real line, whereas within the code they are represented as long double precision floating-point values, with precision of $\pm 10^{-19}$,

moreover the error of the approximate Jordan form computation results in $\delta_{max} < 10^{-17}$. Henceforth we focus on the latter description, as in the main text of this work. The eigen-decomposition of the dynamics is (the values are rounded to three decimal places):

$$A = SJS^{-1} \subseteq \mathbb{S}J\mathbb{S}^{-1} \text{ where}$$

$$\mathbb{S} = \begin{bmatrix} 0.798 \pm 10^{-14} & 0.173 \pm 10^{-15} \\ 0 \pm 10^{-19} & 0.577 \pm 10^{-14} \end{bmatrix}$$

$$J = \begin{bmatrix} 0.985 \pm 10^{-16} & 0.069 \pm 10^{-17} \\ -0.069 \pm 10^{-17} & 0.985 \pm 10^{-16} \end{bmatrix}$$

$$\mathbb{S}^{-1} = \begin{bmatrix} 1.253 \pm 10^{-12} & -0.376 \pm 10^{-13} \\ 0 \pm 10^{-18} & 1.732 \pm 10^{-12} \end{bmatrix}.$$

The discussed over-approximations of the reach-sets indicate that the temperature variable intersects the guard at iteration $\underline{n} = 32$. Considering the pseudo-eigenvalue matrix (described in the extended version for the case of complex eigenvalues) along these iterations, we use Equation (18) to find that the corresponding complex pair remains within the following boundaries:

$$\mathcal{A}^{32} = \begin{bmatrix} r & i \\ -i & r \end{bmatrix} \left\{ \begin{array}{l} 0.4144 < r < 0.985 \\ 0.0691 < i < 0.7651 \\ 0.1082 < r+i < 1.247 \\ 0.9159 < i-r < 0.9389 \end{array} \right.$$

$$\mathcal{B}^{32} = \begin{bmatrix} r & i \\ -i & r \end{bmatrix} \left\{ \begin{array}{l} 1 < r < 13.41 \\ 0 < i < 17.98 \\ 1 < r+i < 29.44 \\ 6.145 < i-r < 6.514 \end{array} \right.$$

The reach tube is calculated by multiplying these abstract matrices with the initial sets of states and inputs, as described in Equation (32), by the following inequalities:

$$\hat{X}_{32}^{\#} = \mathcal{A}^{32} \begin{bmatrix} [5 & 40] \\ [0 & 1] \end{bmatrix} + \mathcal{B}^{32} \begin{bmatrix} [5 & 40] \\ [0 & 300] \end{bmatrix}$$

$$= \begin{bmatrix} temp \\ heat \end{bmatrix} \left\{ \begin{array}{l} -24.76 < temp < 394.5 \\ -30.21 < heat < 253 \\ -40.85 < temp + heat < 616.6 \\ -86.31 < temp - heat < 843.8 \end{array} \right.$$

The negative values represent the lack of restriction in the code on the lower side and correspond to system cooling (negative heating). The set is displayed

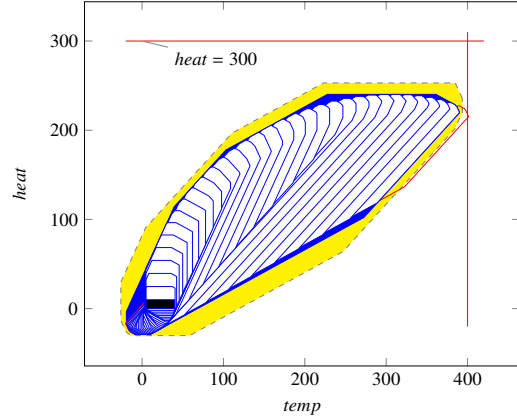


Fig. 9. The abstractly accelerated tube (yellow, dashed boundary), representing an over-approximation of the thermostat reach tube (dark blue). The set of initial conditions is shown in black, whereas successive reach sets are shown in white. The guards and the reach set that crosses them are close to the boundary in red.

in Figure 9, where for the sake of clarity we display only 8 directions of the 16 constraints. This results in a rather tight over-approximation that is not much looser than the convex hull of all reach sets obtained by [20] using the given directions. In Figure 9, we can see the initial set in black colour, the collection of reach sets in white, the convex hull of all reach sets in dark blue (as computed by [20]), and finally the abstractly accelerated set in light yellow (dashed lines). The outer lines represent the guards.

G. Calculating the Number of Iterations for Continuous Dynamics

Following the same steps as in Lemma 3 we develop an equivalent for continuous dynamics.

Lemma 4. *Given a matrix A with eigenvalues $\{\lambda_s \mid s \in [1, r]\}$, where each eigenvalue λ_s has a geometric multiplicity p_s and corresponding gener-*

alised eigenvectors $\{\mathbf{v}_{s,i} \mid i \in [1, p_s]\}$,

$$\begin{aligned} \forall t \geq 0, \mathbf{A}_t \mathbf{v}_s^i &= e^{\lambda_s} \mathbf{v}_{s,i} + \sum_{j=1}^{i-1} t^j e^{\lambda_s} \mathbf{v}_{s,i-j} \\ &= e^{\lambda_s} \left(\mathbf{v}_{s,i} + \sum_{j=1}^{i-1} t^j \mathbf{v}_{s,i-j} \right) \end{aligned} \quad (54)$$

Proof: The proof derives again from the Taylor expansion.

$$\begin{aligned} e^{\mathbf{A}_t} \mathbf{v}_{s,i} &= \sum_{k=0}^{\infty} \mathbf{A}^k \frac{t^k}{k!} \mathbf{v}_{s,i} = \sum_{k=0}^{\infty} \frac{t^k}{k!} (\lambda_s^k \mathbf{v}_{s,i} + k \lambda_s^{k-1} \mathbf{v}_{s,i-1}) \\ &= \sum_{k=0}^{\infty} \frac{t^k}{k!} \lambda_s^k \mathbf{v}_{s,i} + \sum_{k=0}^{\infty} \frac{t^k}{k!} k \lambda_s^{k-1} \mathbf{v}_{s,i-1} \\ &= e^{\lambda_s t} (\mathbf{v}_{s,i} + t \mathbf{v}_{s,i-1}) \end{aligned} \quad (55)$$

The rest of the proof follows the same expansion as in 3 ■

Given the similarity of equation (54) with (52) we may apply exactly the same techniques described in section VI-E to the continuous case.

VII. EXPERIMENTAL RESULTS

The algorithm has been implemented in C++ using the eigen-algebra package (v3.2), with double precision floating-point arithmetic, and has been tested on a 1.6 GHz core 2 duo computer.

A. Comparison with other unbounded-time approaches.

In a first experiment we have benchmarked our implementation against the tools INTERPROC [33] and STING [12]. We have tested these tools on different scenarios, including guarded/unguarded, stable/unstable and complex/real loops with inputs (details in Table I).⁴ It is important to note that in many instances, INTERPROC (due to the limitations of widening) and STING (due to the inexistence of tight polyhedral, inductive invariants) are unable to infer finite bounds at all.

⁴The tool and the benchmarks are available from <http://www.cprover.org/LTI/>.

Table II gives the comparison of our implementation using different levels of precision (long double, 256 bit, and 1024 bit floating-point precision) with the original abstract acceleration for linear loops without inputs (J) [34] (where inputs are fixed to constants). This shows that our implementation gives tighter over-approximations on most benchmarks (column ‘improved’). While on a limited number of instances the current implementation is less precise (Fig. 2 gives a hint why this is happening), the overall increased precision is owed to lifting the limitation on directions caused by the use of logahedral abstractions.

At the same time, our implementation is faster – even when used with 1024 bit floating-point precision – than the original abstract acceleration (using rationals). The fact that many bounds have improved with the new approach, while speed has increased by several orders of magnitude, provides evidence of the advantages of the new approach.

The speed-up is due to the faster Jordan form computation, which takes between 2 and 65 seconds for [34] (using the ATLAS package), whereas our implementation requires at most one second. For the last two benchmarks, the polyhedral computations blow up in [34], whereas our support function approach shows only moderately increasing runtimes. The increase of speed is owed to multiple factors, as detailed in Table III. The difference of using long double precision floating-point vs. arbitrary precision arithmetic is negligible, as all results in the given examples match exactly to 9 decimal places. Note that, as explained above, soundness can be ensured by appropriate rounding in the floating-point computations.

B. Comparison with bounded-time approaches.

In a third experiment, we compare our method with the LGG algorithm [28] used by SPACEEX [20]. In order to set up a fair comparison we have provided the implementation of the native algorithm

name	characteristics				improved		analysis time [sec]		
	type	dim	inputs	bounds	IProc	Sti	IProc	Sti	J+I
parabola_i1	$\neg s, \neg c, g$	2	1	80	+25	+28	0.007	237	0.049
parabola_i2	$\neg s, \neg c, g$	2	1	80	+24	+35	0.008	289	0.072
cubic_i1	$\neg s, \neg c, g$	3	1	120	+44	+50	0.015	704	0.097
cubic_i2	$\neg s, \neg c, g$	3	1	120	+35	+55	0.018	699	0.124
oscillator_i0	$s, c, \neg g$	2	0	56	+24	+24	0.004	0.990	0.021
oscillator_i1	$s, c, \neg g$	2	0	56	+24	+24	0.004	1.060	0.024
inv_pendulum	$s, c, \neg g$	4	0	16	+8	+8	0.009	0.920	0.012
convoyCar2_i0	$s, c, \neg g$	3	2	12	+9	+9	0.007	0.160	0.043
convoyCar3_i0	$s, c, \neg g$	6	2	24	+15	+15	0.010	0.235	0.513
convoyCar3_i1	$s, c, \neg g$	6	2	24	+15	+15	0.024	0.237	0.901
convoyCar3_i2	$s, c, \neg g$	6	2	24	+15	+15	0.663	0.271	1.416
convoyCar3_i3	$s, c, \neg g$	6	2	24	+15	+15	0.122	0.283	2.103

type: s – stable loop, c – complex eigenvalues, g – loops with guard; **dim:** system dimension (variables); **bounds:** nb. of half-planes defining the polyhedral set;

IProc is [33]; **Sti** is [12]; **J+I** is this work;

improved: number of bounds newly detected by J+I over the existing tools (IProc, Sti)

TABLE I
EXPERIMENTAL COMPARISON OF UNBOUNDED-TIME ANALYSIS TOOLS WITH INPUTS

in [28]. We have run both methods on the convoyCar example [34] with inputs, which presents an unguarded, scalable, stable loop with complex dynamics, and focused on octahedral abstractions. For convex reach sets, the approximations computed by abstract acceleration are quite tight in comparison to those computed by the LGG algorithm. However, storing finite disjunctions of convex polyhedra, the LGG algorithm is able to generate non-convex reach tubes, which are arguably more proper in case of oscillating or spiralling dynamics. Still, in many applications abstract acceleration can provide a tight over-approximation of the convex hull of those non-convex reach sets.

Table IV gives the results of this comparison. For simplicity, we present only the projection of the bounds along the variables of interest. As expected, the LGG algorithm performs better in terms of tightness, but its runtime increases with the number of iterations. Our implementation of LGG using Convex Polyhedra with octagonal templates is slower than the abstractly accelerated version even for small time horizons (our implementation of LGG requires

~ 4 ms for each iteration on a 6-dimensional problem with octagonal abstraction). This can be improved by the use of zonotopes, or by careful selection of the directions along the eigenvectors, but this comes at a cost on precision. Even when finding combinations that outperform our approach, this will only allow the time horizon of the LGG approach to be slightly extended before matching the analysis time from abstract acceleration, and the reachable states will still remain unknown beyond the extended time horizon.

The evident advantage of abstract acceleration is its speed over finite horizons without much precision loss, and of course the ability to prove properties for unbounded-time horizons.

C. Scalability

Finally, in terms of scalability, we have an expected $O(n^3)$ complexity worst-case bound (from the matrix multiplications in equation (32)). We have parameterised the number of cars in the convoyCar example [34] (also seen in Table II), and experimented with up to 33 cars (each car after

name	characteristics			improved		analysis time (sec)					
	type	dim	bounds	tighter	looser	J (jcf)		mpfr+(jcf)		mpfr	ld
parabola_i1	$\neg s, \neg c, g$	3	80	+4(5%)	0(0%)	2.51	(2.49)	0.16	(0.06)	0.097	0.007
parabola_i2	$\neg s, \neg c, g$	3	80	+4(5%)	0(0%)	2.51	(2.49)	0.26	(0.06)	0.101	0.008
cubic_i1	$\neg s, \neg c, g$	4	120	0(0%)	0(0%)	2.47	(2.39)	0.27	(0.20)	0.110	0.013
cubic_i2	$\neg s, \neg c, g$	4	120	0(0%)	0(0%)	2.49	(2.39)	0.32	(0.20)	0.124	0.014
oscillator_i0	$s, c, \neg g$	2	56	0(0%)	-1(2%)	2.53	(2.52)	0.12	(0.06)	0.063	0.007
oscillator_i1	$s, c, \neg g$	2	56	0(0%)	-1(2%)	2.53	(2.52)	0.12	(0.06)	0.078	0.008
inv_pendulum	$s, c, \neg g$	4	12	+8(50%)	0(0%)	65.78	(65.24)	0.24	(0.13)	0.103	0.012
convoyCar2_i0	$s, c, \neg g$	5	12	+9(45%)	0(0%)	5.46	(4.69)	3.58	(0.22)	0.258	0.005
convoyCar3_i0	$s, c, \neg g$	8	24	+10(31%)	-2(6%)	24.62	(11.98)	3.11	(1.01)	0.552	0.051
convoyCar3_i1	$s, c, \neg g$	8	24	+10(31%)	-2(6%)	23.92	(11.98)	4.94	(1.01)	0.890	0.121
convoyCar3_i2	$s, c, \neg g$	8	24	+10(31%)	-2(6%)	1717.00	(11.98)	6.81	(1.01)	1.190	0.234
convoyCar3_i3	$s, c, \neg g$	8	24	+10(31%)	-2(6%)	1569.00	(11.98)	8.67	(1.01)	1.520	0.377

type: s – stable loop, c – complex eigenvalues, g – loops with guard; **dim:** system dimension (including fixed inputs); **bounds:** nb. of half-planes defining the polyhedral set; **improved:** number of bounds (and percentage) that were tighter (better) or looser (worse) than [34];

J is [34]; **mpfr+** is this article using 1024bit mantissas ($e < 10^{-152}$); **mpfr** uses a 256bit mantissa ($e < 10^{-44}$); **ld** uses a 64bit mantissa ($e < 10^{-11}$); here e is the accumulated error of the dynamical system; **jcf:** time taken to compute Jordan form

TABLE II
EXPERIMENTAL COMPARISON WITH PREVIOUS WORK

the first requires 3 variables, so that for example $(33 - 1) \times 3 = 96$ variables), and have adjusted the initial states/inputs sets. We report an average of 10 runs for each configuration. These results demonstrate that our method scales to industrial-size problems.

# of variables	3	6	12	24	48	96
runtime (s)	0.004	0.031	0.062	0.477	5.4	56

VIII. RELATED WORK

There are several approaches that solve the safety problem for the linear and other cases such as hybrid systems. They are broadly divided into two categories due to the inherent nature of these. Namely

Optimisation	Speed-up
Eigen vs. ATLAS ⁵	2–10
Support functions vs. generators	2–40
long double vs. multiple precision arithmetic	5–200
interval vs. regular arithmetic	.2–.5
Total	4–80000

TABLE III
PERFORMANCE IMPROVEMENTS BY FEATURE

the time bounded analysis is in most cases unsound since it cannot reason about the unbounded time case (we note that a proof of the existence of a fix-point for the given horizon would restore such soundness by many tools do not attempt to find such proof which is left to the user). Unbounded-time solutions are therefore preferred when such soundness is required, although they are often either less precise or slower than their bounded counterparts.

A. Time-Bounded Reachability Analysis

The first approach is to surrender exhaustive analysis over the infinite time horizon, and to restrict the exploration to system dynamics up to some given finite time bound. Bounded-time reachability is decidable, and decision procedures for the resulting satisfiability problem have made much progress in the past decade. The precision related to the bounded analysis is offset by the price of uncertainty: behaviours beyond the given time bound are not considered, and may thus violate a safety requirement. Representatives are STRONG [15], HySon [7],

name	this article		LGG		
	100 iterations	unbounded	100 iterations	200 iterations	300 iterations
run time	166 ms	166 ms	50 ms	140 ms	195 ms
car acceleration	[-0.820 1.31]	[-1.262 1.31]	[-0.815 1.31]	[-0.968 1.31]	[-0.968 1.31]
car speed	[-1.013 5.11]	[-4.515 6.15]	[-1.013 4.97]	[-3.651 4.97]	[-3.677 4.97]
car position	[43.7 83.4]	[40.86 91.9]	[44.5 83.4]	[44.5 88.87]	[44.5 88.87]

TABLE IV
COMPARISON ON CONVOYCAR2 BENCHMARK, BETWEEN THIS WORK AND THE LGG ALGORITHM [28]

CORA [1], HYLAA [3] and SpaceEx [20].

Set-based simulation methods generalise guaranteed integration [6], [37] from enclosing intervals to relational domains. They use precise abstractions with low computational cost to over-approximate sets of reachable states up to a given time horizon. Early tools used polyhedral sets (HyTECH [31] and PHAVER [19]), polyhedral flow-pipes [10], ellipsoids [5] and zonotopes [24]. A breakthrough was achieved by [25], [28], with the representation of convex sets using template polyhedra and support functions. This method is implemented in the tool SPACEEX [20], which can handle dynamical systems with hundreds of variables. Although it may use exact arithmetic to maintain soundness, it performs computations using floating-point numbers: this is a deliberate choice to boost performance, which, although quite reasonable, its implementation is numerically unsound and therefore does not provide genuine formal guarantees. In fact, most tools using eigendecomposition over a large number of variables (more than 10) are numerically unsound due to the use of unchecked floating-point arithmetic. Another breakthrough in performance was done by HYLAA [3] which was the first tool to solve all high order problems of hundreds and thousands dimensions. Other approaches use specialised constraint solvers (HySAT [18], iSAT [16]), or SMT encodings [11], [29] for bounded model checking of hybrid automata.

B. Unbounded Reachability Analysis

The second approach, epitomised in static analysis methods [30], explores unbounded-time horizons. It employs conservative over-approximations to achieve completeness and decidability over infinite time horizons.

Unbounded techniques attempt to infer a *loop invariant*, i.e., an inductive set of states that includes all reachable states. If the computed invariant is disjoint from the set of bad states, this proves that the latter are unreachable and hence that the loop is safe. However, analysers frequently struggle to obtain an invariant that is precise enough with acceptable computational cost. The problem is evidently exacerbated by non-determinism in the loop, which corresponds to the case of open systems. Prominent representatives of this analysis approach include Passel [35], Sting [12], and abstract interpreters such as ASTRÉE [4] and InterProc [33]. Early work in this area has used implementations of abstract interpretation and widening [13], which are still the foundations of most modern tools. The work in [30] uses abstract interpretation with convex polyhedra over piecewise-constant differential inclusions. Dang and Gawlitza [14] employ optimisation-based (max-strategy iteration) with linear templates for hybrid systems with linear dynamics. Relational abstractions [38] use ad-hoc “loop summarisation” of flow relations, while abstract acceleration focuses on linear relations analysis [26], [27], which is common in program analysis.

C. Abstract Acceleration

Abstract acceleration [26], [27], [34] captures the effect of an arbitrary number of loop iterations with a single, non-iterative transfer function that is applied to the entry state of the loop (i.e., to the set of initial conditions of the linear dynamics). Abstract acceleration has been extended from its original version to encompass inputs over reactive systems [40] but restricted to subclasses of linear loops, and later to general linear loops but without inputs [34].

The work presented in this article lifts these limitations by presenting abstract acceleration for *general* linear loops *with* inputs [8], developing numeric techniques for scalability and extending the domain to continuous time systems.

IX. CONCLUSIONS AND FUTURE WORK

We have presented an extension of the Abstract Acceleration paradigm to guarded LTI systems (linear loops) with inputs, overcoming the limitations of existing work dealing with closed systems. We have decisively shown the new approach to over-compete state-of-the-art tools for unbounded-time reachability analysis in both precision and scalability. The new approach is capable of handling general unbounded-time safety analysis for large scale open systems with reasonable precision and fast computation times. Conditionals inside loops and nested loops are out of the scope of this paper.

Work to be done is extending the approach to non-linear dynamics, which we believe can be explored via hybridisation techniques [2], and to formalise the framework for general hybrid models with multiple guards and location-dependent dynamics, with the aim to accelerate transitions across guards rather than integrate individual accelerations on either side of the guards.

a) **ACKNOWLEDGMENTS.**: We would like to thank Colas Le Guernic for his constructive suggestions and comments on the paper.

REFERENCES

- [1] M. Althoff. An introduction to cora 2015. In *ARCH@ CPSWeek*, pages 120–151, 2015.
- [2] E. Asarin, T. Dang, and A. Girard. Hybridization methods for the analysis of nonlinear systems. *Acta Informatica*, 43(7):451–476, 2007.
- [3] S. Bak and P. S. Duggirala. Hylaa: A tool for computing simulation-equivalent reachability for linear systems. In *Proceedings of the 20th International Conference on Hybrid Systems: Computation and Control, HSCC 2017, Pittsburgh, PA, USA, April 18-20, 2017*, pages 173–178, 2017.
- [4] B. Blanchet, P. Cousot, R. Cousot, J. Feret, L. Mauborgne, A. Miné, D. Monniaux, and X. Rival. A static analyzer for large safety-critical software. In *PLDI*, pages 196–207. ACM, 2003.
- [5] O. Botchkarev and S. Tripakis. Verification of hybrid systems with linear differential inclusions using ellipsoidal approximations. In *HSCC, LNCS*, pages 73–88. Springer, 2000.
- [6] O. Bouissou. *Analyse statique par interprétation abstraite de systèmes hybrides*. PhD thesis, École Polytechnique, 2008.
- [7] O. Bouissou, S. Mimram, and A. Chapoutot. Hyson: Set-based simulation of hybrid systems. In *Rapid System Prototyping (RSP), 2012 23rd IEEE International Symposium on*, pages 79–85. IEEE, 2012.
- [8] D. Cattaruzza, A. Abate, P. Schrammel, and D. Kroening. Unbounded-time analysis of guarded LTI systems with inputs by abstract acceleration. In *SAS*, volume 9291 of *LNCS*, pages 312–331. Springer, 2015.
- [9] D. Cattaruzza, A. Abate, P. Schrammel, and D. Kroening. Sound numerical computations in abstract acceleration. In *International Workshop on Numerical Software Verification*, pages 38–60. Springer, 2017.
- [10] A. Chutinan and B. H. Krogh. Computing polyhedral approximations to flow pipes for dynamic systems. In *CDC*, pages 2089–2094. IEEE Computer Society, 1998.
- [11] A. Cimatti, S. Mover, and S. Tonetta. SMT-based verification of hybrid systems. In *AAAI Conference on Artificial Intelligence*. AAAI Press, 2012.
- [12] M. A. Colón, S. Sankaranarayanan, and H. B. Sipma. Linear invariant generation using non-linear constraint solving. In *CAV*, pages 420–432. Springer, 2003.
- [13] P. Cousot and R. Cousot. Abstract interpretation: A unified lattice model for static analysis of programs by construction or approximation of fixpoints. In *POPL*, pages 238–252, 1977.
- [14] T. Dang and T. M. Gawlitza. Template-based unbounded time verification of affine hybrid automata. In *APLAS, LNCS*, pages 34–49. Springer, 2011.
- [15] Y. Deng, A. Rajhans, and A. A. Julius. STRONG: A trajectory-based verification toolbox for hybrid systems. In

- Quantitative Evaluation of Systems*, volume 8054 of *LNCS*, pages 165–168. Springer, 2013.
- [16] A. Eggers, M. Fränzle, and C. Herde. SAT Modulo ODE: A direct SAT approach to hybrid systems. In *ATVA*, volume 5311 of *LNCS*, pages 171–185. Springer, 2008.
- [17] A. Fehnker and F. Ivancic. Benchmarks for hybrid systems verification. In *HSCC*, pages 326–341. Springer, 2004.
- [18] M. Fränzle and C. Herde. HySAT: An efficient proof engine for bounded model checking of hybrid systems. *Formal Methods in System Design*, 30(3):179–198, 2007.
- [19] G. Frehse. PHAVer: Algorithmic verification of hybrid systems past HyTech. In *HSCC*, volume 3414 of *LNCS*, pages 258–273. Springer, 2005.
- [20] G. Frehse, C. L. Guernic, A. Donzé, R. Ray, O. Lebeltel, R. Ripado, A. Girard, T. Dang, and O. Maler. SpaceEx: Scalable verification of hybrid systems. In *CAV*, volume 6806 of *LNCS*, pages 379–395. Springer, 2011.
- [21] K. Fukuda and A. Prodon. Double description method revisited. In *Combinatorics and computer science*, pages 91–111. Springer, 1996.
- [22] S. Gao, J. Avigad, and E. M. Clarke. δ -complete decision procedures for satisfiability over the reals. In *Automated Reasoning*, pages 286–300. Springer, 2012.
- [23] P. K. Ghosh and K. V. Kumar. Support function representation of convex bodies, its application in geometric computing, and some related representations. *Computer Vision and Image Understanding*, 72:379–403, 1998.
- [24] A. Girard. Reachability of uncertain linear systems using zonotopes. In *HSCC*, volume 3414 of *LNCS*, pages 291–305. Springer, 2005.
- [25] A. Girard, C. L. Guernic, and O. Maler. Efficient computation of reachable sets of linear time-invariant systems with inputs. In *HSCC*, volume 3927 of *LNCS*, pages 257–271. Springer, 2006.
- [26] L. Gonnord and N. Halbwegs. Combining widening and acceleration in linear relation analysis. In *SAS*, LNCS, pages 144–160. Springer, 2006.
- [27] L. Gonnord and P. Schrammel. Abstract acceleration in linear relation analysis. *Science of Computer Programming*, 93(Part B):125–153, 2014.
- [28] C. L. Guernic and A. Girard. Reachability analysis of hybrid systems using support functions. In *CAV*, volume 5643 of *LNCS*, pages 540–554. Springer, 2009.
- [29] S. Gulwani and A. Tiwari. Constraint-based approach for analysis of hybrid systems. In *CAV*, volume 5123 of *LNCS*, pages 190–203. Springer, 2008.
- [30] N. Halbwegs, P. Raymond, and Y.-E. Proy. Verification of linear hybrid systems by means of convex approximations. In *SAS*, volume 864 of *LNCS*, pages 223–237. Springer, 1994.
- [31] T. A. Henzinger, P.-H. Ho, and H. Wong-Toi. HyTech: A model checker for hybrid systems. *Journal on Software Tools for Technology Transfer*, 1(1-2):110–122, 1997.
- [32] R. A. Horn and C. R. Johnson. *Matrix analysis*. Cambridge university press, 2012.
- [33] B. Jeannet. Interproc analyzer for recursive programs with numerical variables, 2010. <http://pop-art.inrialpes.fr/interproc/interprocweb.cgi>.
- [34] B. Jeannet, P. Schrammel, and S. Sankaranarayanan. Abstract acceleration of general linear loops. In *POPL*, pages 529–540. ACM, 2014.
- [35] T. T. Johnson and S. Mitra. Passel: A verification tool for parameterized networks of hybrid automata, 2012. <https://publish.illinois.edu/passel-tool/>.
- [36] P. Lancaster and M. Tismenetsky. *The Theory of Matrices*. Academic Press, 2nd edition, 1984.
- [37] R. Löhner. *Einschließung der Lösung gewöhnlicher Anfangs- und Randwertaufgaben und Anwendungen*. PhD thesis, Universität Karlsruhe, 1988.
- [38] S. Sankaranarayanan and A. Tiwari. Relational abstractions for continuous and hybrid systems. In *CAV*, volume 6806 of *LNCS*, pages 686–702. Springer, 2011.
- [39] P. Schrammel. Unbounded-time reachability analysis of hybrid systems by abstract acceleration. In *Embedded Software*, pages 51–54. IEEE, 2015.
- [40] P. Schrammel and B. Jeannet. Applying abstract acceleration to (co-)Reachability analysis of reactive programs. *Journal of Symbolic Computation*, 47(12):1512–1532, 2012.